Investigating the energy yield of rain cells

William Nævdal Sigurdsson

Master's Thesis in Measurement Science

Supervisor: Prof. Lars Egil Helseth
Co-supervisor: Dr. Martin Møller Greve

Department of Physics and Technology

University of Bergen

November 2018

UNIVERSITY OF BERGEN

Abstract

Faculty of Mathematics and Natural Sciences
Department of Physics and Technology

Master of Science

Investigating the energy yield of rain cells

by William Nævdal Sigurdsson

Harvesting energy from rain has been done indirectly for hundreds of years by building dams or reservoirs. Recently, research has been made into gathering energy from individual raindrops. One of the discovered methods make use of the triboelectric effect taking place when rain drops land on a hydrophobic polymer. Electrical charge is induced in interdigitated electrodes beneath the polymer, and a voltage is induced between them. This thesis uses a simple model to describe the electrical behaviour of such a rain cell, and evaluates the energy harvesting potential it represents. Power measurements for different resistive loads are taken to determine the effective capacitance of the rain cell. A model for the charging and discharging of a storage capacitor through a full wave rectifier is developed and compared with experiment. The power and charge delivered by a raindrop are derived and a model relating the energy storage to the rain intensity is created and used to evaluate the limits of the rain cell.

Acknowledgements

I would like to thank my advisors Prof. Lars Egil Helseth and Dr. Martin Møller Greve for giving generously of their time, and giving excellent advice.

I would also like to thank Stine, for always putting up with me.

Contents

List of Figures

List of Tables

List of Abbreviations

AC	**A**lternating **C**urrent
DC	**D**irect **C**urrent
RF	**R**adio **F**requency
PTFE	**P**oly**T**etra**F**luoro**E**thylene
PET	**P**oly**E**thylene**T**erephtalate
FEP	**F**luroinated **E**thylene **P**ropylene
ITO	**I**ndium **T**in **O**xide

For/Dedicated to/To my...

Chapter 1

Introduction

1.1 Background

1.1.1 Energy harvesting

The advent of smart homes, Internet of Things, and remote operation has brought with it the need for sensors capable of operating for long periods of time without energy refills. Battery capacity has increased greatly over the last decades, but in certain circumstances even a long-lasting battery is insufficient. Energy harvesting technology fills this need, allowing for the localized gathering of energy and giving electronic devices self-sufficiency energy-wise.

There are several methods in use for transducing various forms of ambient energy into usable electrical energy. Perhaps most well known is solar power, which transforms light energy into electrical energy through the photo-voltaic effect. This technology spans from the powering of the International Space Station to pocket calculators to entire cities [1]. Where there exists a temperature differential, it is possible to utilize the Seebeck effect to create a DC voltage[2]. Some materials have piezoelectric properties, meaning that they generate electricity when they are subjected to mechanical stress (and vice versa). These materials can be used in vibration transducers or wherever there is predictable mechanical motion. Recently there have been developments in human-powered energy harvesting systems, where human movement provides the energy. Piezoelectric materials are typically used in these applications[3]. Radio waves in in the air have some energy, and with an antenna that energy can be exploited. Old crystal radios had no internal power source, relying only on the power of the RF signals to make sound. However, the need for tuning and the low energy density means that RF energy harvesting is often only viable in cases with directed RF signals, not ambient waves[4]. [5]

For low-power energy harvesters, there is often not enough energy available to continuously drive a load. They can, however, be used intermittently. For instance, an energy harvesting system can gather energy over the period of a day, and gather

enough to power a microcontroller and a sensor for a few seconds, enough to make a measurement and transmit it.

Rain energy is a relatively new field of study. Historically, water energy has been focused toward big reservoirs and large scale energy production[]. Rainfall over a substantial area is collected into magazines and water flow from this magazine will usually turn a turbine and produce electricity. This philosophy is not well-suited for small, autonomous sensors as it requires too much real-estate. Additionally, having fewer moving parts means less need for maintenance and repair, which is beneficial for a sensor that is supposed to function on its own.

There has been some research into gathering power from individual raindrops by them hitting piezoelectric transducers. However, a new method of harvesting this energy has been developed, taking advantage of the properties of hydrophobic materials and the triboelectric effect.

1.1.2 The rain cell

The triboelectric nanogenerator was first conceived by Prof. Zhong Lin Wang's group at Georgia Institute of Technology [6]. When two different materials come into contact, opposite electrical charges will form on their surfaces. Some of this charge remains when the materials are pulled apart again, creating a voltage difference between the two surfaces. This basic mechanical to electrical transduction has been applied to different systems [7]. It was shown that this is possible using water in the form of liquid waves [8], and finally triboelectrically induced raindrop energy was demonstrated in a solar/rain hybrid cell by Zheng et al. [9].

This hybrid cell consisted of a hydrophobic polymer called polytetrafluoroethylene (PTFE) on top of a indium tin oxide (ITO) electrode. In this study the droplets were thought to be charged through contact electrification by air or airborne particles, and as droplets periodically landed on the polymer and fell off, there would be an alternating potential difference. In another article, the polymer itself was also mentioned as a possible source for triboelectric charging [10].

Yang and Halvorsen examined the power generation capability of a rolling conductive droplet on a charged PTFE electret, with two interdigital electrodes underneath [11, 12].

Helseth and Guo used fluorinated ethylene propylene (FEP) as the hydrophobic polymer [13, 14, 15], and also explored the use of interdigital grating electrodes [16]. It is this iteration, with a FEP polymer charged triboelectrically by impinging water droplets, and alternating current created by rolling or sliding droplets over

the electrodes, that is the starting point of this thesis.

The triboelectric rain cell consists of a hydrophobic polymer lying on top of a conductive electrode. When rain drops fall onto the polymer and slide off, negative electrical charge is imparted onto the surface through contact electrification. Eventually, the whole of the hydrophobic surface holds some negative charge, and positive charge is electrostatically induced in the electrode. As additional droplets fall onto the polymer, positive charge is induced in them as well, and as they roll over the electrode, a small alternating current goes through the electrode.

1.1.3 Uses for rain cells

There are many potential uses for rain cell energy. As previously mentioned, the powering of autonomous sensors is in increasing demand. In areas with more rain than sun, rain cells could be a viable alternative to solar panels. Within digital microfluidics, droplet energy has been used to power actuation systems [17]. As demonstrated by Wang's group [9], the transparent nature of many hydrophobic polymers mean that they can be attached to the outside of solar panels without drastically reducing the capability of the solar panel. This makes it possible for rain cells and solar panels to work in conjunction, with one taking over when the other stops working, or both operating at the same time.

1.2 Thesis objectives and outline

The motive for this thesis is to evaluate the energy gathering potential of the proposed triboelectric rain cell, and

Her bør du skrive en god del mer: det må være klart og tydelig hva som er målet med oppgaven. Dette er veldig viktig!

The main objective of this thesis is twofold. First the electrical characteristics of a model rain cell are investigated as a function of time and resistive load, and models are developed to allow one understand these data. Second, a scheme to rectify the current and store the electrical energy is investigated experimentally, and a new model is developed to understand how the charge builds up in the storage capacitor as time passes.

As triboelectric material for the rain droplets, a 25 um thick fluorinated ethylene propylene (FEP) polymer film is used. Interdigitated aluminium or nickel electrodes of about 100 nm thickness are evaporated onto the back-side of the FEP using a electron-beam evaporator located at the nanolaboratory at the Department of Physics and Technology, and external electrical wires were connected to the electrodes using conducting glue or tape.

In this thesis, the current and voltage was monitored as water droplets of fized size dropped onto the FEP surface. A new analytical model was developed to evaluate how the time-dependent electrical signal would look like. Fits of the model indicated good agreement with the experimental data.

The electrical power was measured as function of resistive load, and a model developed was to explain this behavior.

A bridge rectifier and a capacitor was used to rectify and store the electrical signal from the rain cell.

Finally this behaviour was extrapolated to real world scenarios, and tied up to rain intensity.

Chapter 2

Background and theory

2.1 Hydrophobic materials

Hydrophobic materials have a reduced level of attraction to water, and vice versa. As the polar molecules of water tend to stick to each other, water will seemingly be repelled to some degree by the hydrophobic material. Therefore, water lying on a hydrophobic surface will draw itself into a drop, and if the surface is inclined, the drop will easily move with a low coefficient of friction and a smaller contact area. The ability of a material to maintain contact with the liquid lying on top of it is referred to as wettability. Wettability is the inverse property of hydrophobicity and is usually quantified by the contact angle where the three phases air, liquid and solid meet [18]. Large contact angles imply low levels of wettability, which in turn means high hydrophobicity.

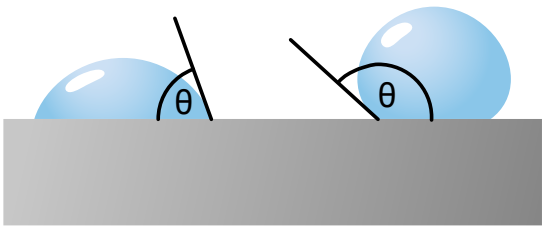

FIGURE 2.1: Contact angles for hydrophilic and hydrophobic materials

FEP is a common fluoroplymer with hydrophobic capabilites. The contact angle between FEP and deionized water is about 109° [13]. Its molecular structure is quite similar to PTFE, but FEP is melt-processible which makes it possible to process different structures in the surface [14]. FEP in a thin-film form will transmit 96% of inbound light [19], which makes it suitable for smart windows or working with

solar panels. Most importantly, FEP has a high density of fluorine atoms, which allows for increased charge transfer by means of the triboelectric effect [14].

2.2 Rain cell mechanics

It has been demonstrated that when pure water droplets slide or roll over a hydrophobic surface, the surface tends to get a negative charge, and the drop tends to retain a positive charge [20]. Exactly why the water interfaces with air or hydrophobic surfaces has this intrinsic negative charge has been the matter of some discussion.[21] While a universal consensus remains to be achieved, significant evidence suggests that preferential adsorption and/or orientation of OH groups near the hydrophobic polymer surface is the cause of this negative charge [21][22][23].

The rain cell consists of a hydrophobic polymer on top of a pair of interdigitated electrodes at some angle. As a rain droplet falls onto the polymer, the surface is triboelectrically charged, and an electric double layer forms. As the droplet down off the polymer, it gains positive charge, while negative charge is left behind on the polymer surface. When the droplet has fallen off, a net negative charge remains along its track. More raindrops follow, and as they take different paths on the rain cell, more of its surface area gains negative charge. At some point, the whole surface is presumably charged. Positive charge in the electrodes are drawn to the charges on the surface, and an equilibrium forms. As the whole surface has similar charge density and the electrodes have the same area, there is no voltage between the electrodes.

As more droplets fall onto the charged surface, positively charged ions within them are drawn to the negatively charged surface, creating an electrical double layer. When the droplet rolls over the edge of an electrode, the positive charge in the droplet disturbs the equilibrium, and positive charge in the electrode is repulsed. As the whole drop passes on top of the electrode a new equilibrium is formed. At this point, if the electrodes are not connected, there exists a voltage difference between them. The droplet will keep moving, and roll over the other edge of the electrode again. The positive charge in the electrode are no longer repelled by the positive charge in the droplet, and flow back to the original equilibrium. The droplet then rolls onto the other electrode and the same procedure occurs, but with the voltage between the electrodes reversed.

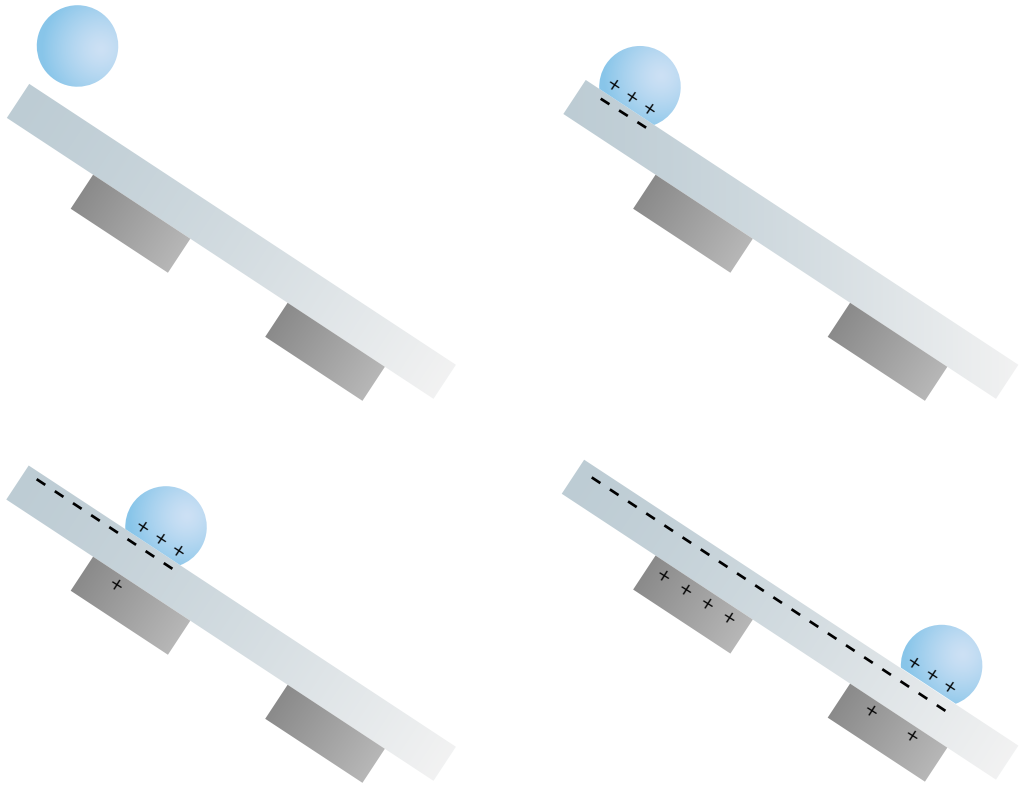

FIGURE 2.2: Stages of contact electrification

An alternating voltage between the electrodes is produced as the droplet rolls down the surface and electrostatically inducing charge in alternating electrodes. The magnitude of this voltage depends on the amount of charge the droplet is able to to induce in the electrode, which in turn depends on how charged the polymer surface is. This voltage can produce a current, which can be rectified into DC and subsequently stored.

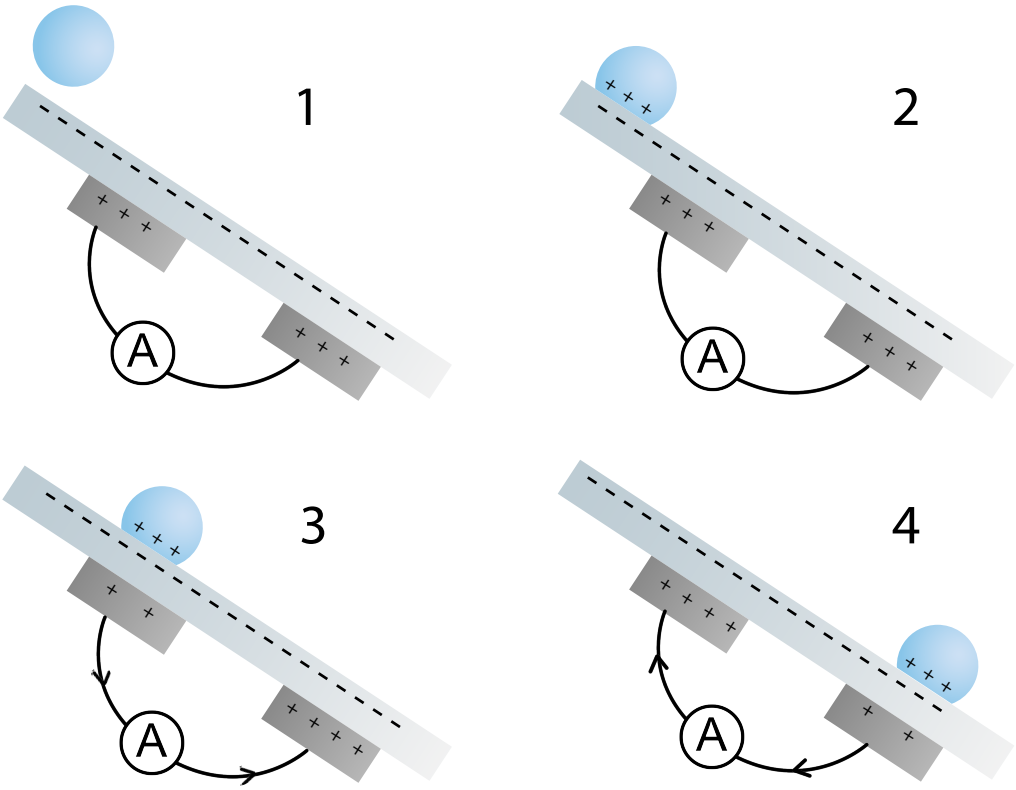

FIGURE 2.3: The positive charge in the raindrop induces a current between the electrodes

A pulse of voltage will also typically be created whenever a droplet lands on the grid part of the rain cell. The droplet will be deformed by gravity as it lands, and unless it lands perfectly and covers both electrodes with the same amount of charge, a voltage is electrostatically induced. The magnitude of this voltage depends on how the drop lands in respect to the two electrodes.

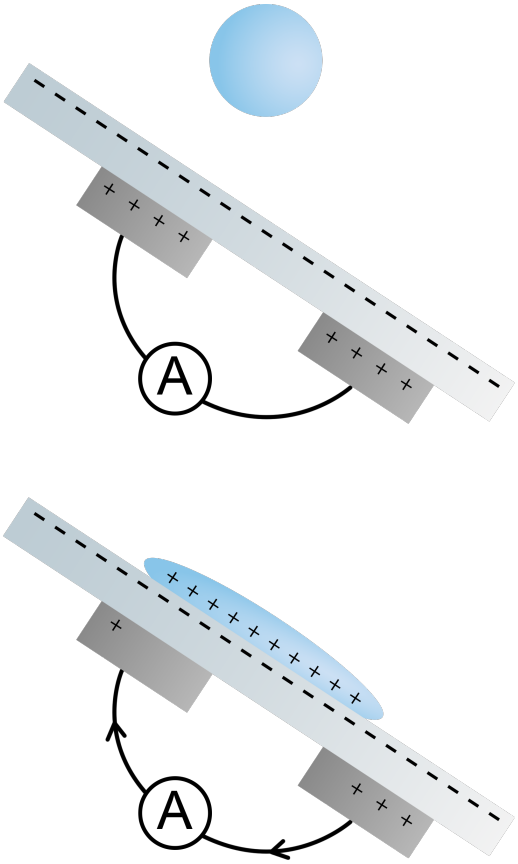

FIGURE 2.4: Second mode of voltage induction. A droplet is flattened unevenly over the electrodes and induces charge unevenly, causing a current

2.3 Waveform characteristics

As explained in section 2.2 there are two modes of voltage generation, impact and rolling/sliding. The construction of the rain cell will have some say in the dominance of each mode.

Since the charge distribution in the polymer is considered constant after sufficient wetting, the charge induction in the electrodes is directly dependent on the intersection of the droplet and electrode surface area [16]. The rate of change in intersecting surface area is therefore proportional to the current $I = dq/dt$. For the sake of simplicity, the charge density of the droplet is assumed to be constant and uniform, and the droplet is assumed to be circular.

$$I = \frac{dq}{dt} = \sigma \frac{dA}{dt} \tag{2.1}$$

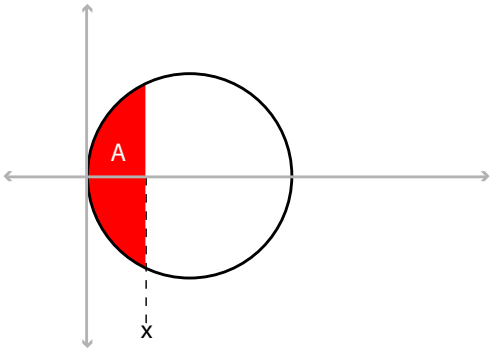

FIGURE 2.5: Area of intersection

The sector area for a raindrop with radius R (figure 2.5):

$$y = \sqrt{R^2 - (x - R)^2} \tag{2.2}$$

The area is found by integrating from 0 to x covering the red-shaded sector in fig. 2.5

$$A = 2\int_0^x \sqrt{R^2 - (x - R)^2}dx \tag{2.3}$$

The current is found by using equation 2.1. This is the current as the droplet rolls onto the first finger.

$$I(t) = \sigma\frac{dA}{dt} = \sigma\frac{dA}{dx}\frac{dx}{dt} = 2\sqrt{R^2 - (x - R)^2}\frac{dx}{dt} \tag{2.4}$$

The velocity is given by v(t)=dx/dt, and the position is given by the integral over the time interval t_0 to t, where t_0 is the time as the droplet rolls onto the first electrode finger.

$$I(t) = 2\sigma v(t)\sqrt{R^2 - \left(\int_{t_0}^{t} v(t)dt - R\right)^2} \tag{2.5}$$

If the velocity of the droplet is approximately constant, this can be simplified.

$$I(t) = 2\sigma v\sqrt{R^2 - (vt - R)^2} \tag{2.6}$$

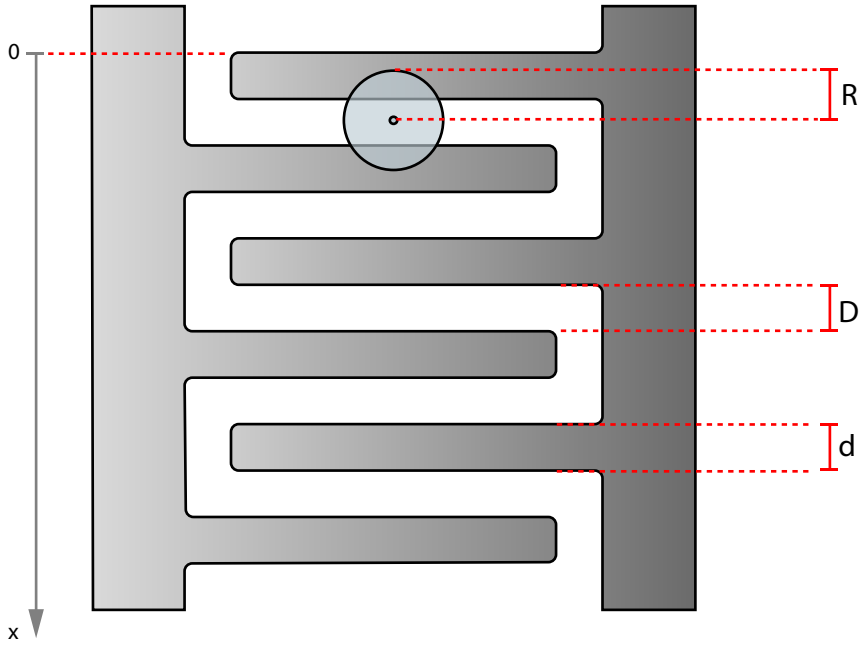

FIGURE 2.6: Raincell geometry

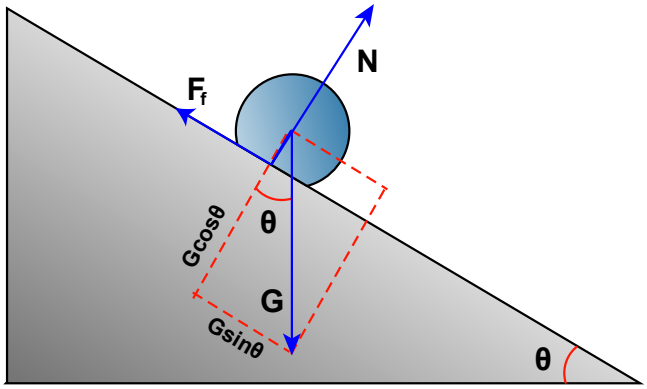

FIGURE 2.7: Simple model of a droplet on a ramp

$G = mg$ Gravitational force

$N = G\cos\theta$ Normal force

$F_f = \mu N$ Friction

$F = G\sin\theta$ Force in direction of movement

$g = 9.81m/s^2$ Standard acceleration due to gravity

μ Coefficient of friction

Newtons 2nd law gives, using the forces presented in fig. 2.7:

$$m\frac{d^2x}{dt^2} = mg\sin\theta - \mu mg\cos\theta \tag{2.7}$$

Upon integrating eq. (2.9), the velocity becomes

$$v(t) = g(\sin\theta - \mu\cos\theta)t = \xi t \tag{2.8}$$

The current in this case is then:

$$I(t) = 2\sigma\xi t\sqrt{R^2 - \left(\frac{\xi t^2}{2} - R\right)^2} \tag{2.9}$$

Where ξ is $g(\sin\theta - \mu\cos\theta)$.

Given the rain cell model of a capacitor being delivered a current, the voltage can be derived in a similar manner.

$$V = \frac{Q}{C} = \sigma\frac{A}{C} \tag{2.10}$$

$$A = 2\int_0^x \sqrt{R^2 - (x-R)^2}dx \tag{2.11}$$

$$V = \frac{2\sigma}{C}\int_0^t v(t)\sqrt{R^2 - (x(t)-R)^2}dt \tag{2.12}$$

$$V(t) = \frac{2\sigma}{C}\int_0^t \xi t\sqrt{R^2 - \left(\frac{\xi t^2}{2} - R\right)^2}dt \tag{2.13}$$

For an interdigitated rain cell with electrodes having N digits each, the cumulative equation is as follows:

$$V = \frac{2\sigma}{C}\sum_{i=1}^{N}(-1)^{\frac{i(i+3))}{2}}\int_0^t \xi t\sqrt{R^2 - \left(\frac{\xi t^2}{2} - R - \left[\frac{2i-3-(-1)^i}{4}\right]D - \left[\frac{2i-1+(-1)^i}{4}\right]d\right)^2}dt \tag{2.14}$$

The current:

$$I = 2\sigma\sum_{i=1}^{N}(-1)^{\frac{i(i+3))}{2}}\xi t\sqrt{R^2 - \left(\frac{\xi t^2}{2} - R - \left[\frac{2i-3-(-1)^i}{4}\right]d - \left[\frac{2i-1+(-1)^i}{4}\right]D\right)^2} \tag{2.15}$$

As the rain cell produces very little power, the loading properties of the multimeter and leakage through the diodes start to play a part. This loss can be modeled as a high value resistor.

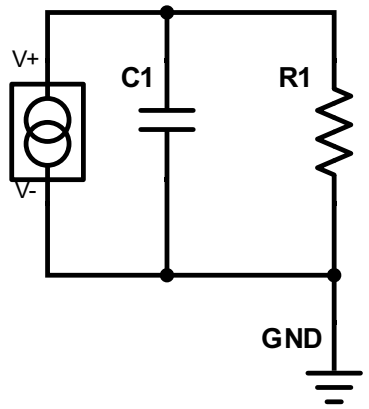

FIGURE 2.8: Current source model of rain cell

$$I = I_C + I_R \tag{2.16}$$

$$I(t) = C\frac{dV(t)}{dt} + \frac{V(t)}{R} \tag{2.17}$$

$$\frac{dV(t)}{dt} = -\frac{V(t)}{RC} + \frac{I(t)}{C} \tag{2.18}$$

The solution to this differential equation:

$$V(t) = e^{-\frac{t}{RC}} \int_0^t \frac{e^{\frac{x}{RC}}\, I(x)}{C} dx \tag{2.19}$$

2.3.1 Power transfer

For a circuit to transfer the maximum amount of power, the Thévenin impedance of the circuit needs to be matched to the load impedance [24] p380. The max power transfer occurs when the load impedance is the complex conjugate of the circuits output impedance.

$$Z_L = Z_{Th}^* \tag{2.20}$$

Taking this approach with the rain cell is complicated by a couple of factors. First of all, Thévenin equivalents only hold true for linear circuits, of which there is no guarantee the rain cell is one. Furthermore, the impedance of the rain cell will vary as droplets interact with it. Also, the produced waveform is not fully sinusoidal, which makes impedance calculations a lot more troublesome.

However, treating the signal as if it is sinusoidal is beneficial, in that it allows us to narrow down the range of impedances that will yield the best power transfer from the rain cell.

Assuming the rain cell produces a somewhat sinusoidal waveform, the power transmission with a resistive load is calculated as a voltage divider:

$$\frac{|V|R}{|Z_C + R_L|} = |V_R| \tag{2.21}$$

$$\frac{|V|^2 R}{|Z_C + R_L|^2} = \frac{|V_R|^2}{R} = |P| \tag{2.22}$$

$$|P| = \frac{|V|^2 R}{X_C^2 + R_L^2} \tag{2.23}$$

$$|P| = \frac{|V|^2 R}{\frac{1}{\omega C}^2 + R_L^2} \tag{2.24}$$

The max power transfer when the load is purely resistive is given by the following formula [24]:

$$R_L = \sqrt{R_{Th}^2 + (X_L + X_C)^2} \tag{2.25}$$

Considering the rain cell model of a source and a capacitor, this is simplified:

$$R_{max\ power} = X_C = \frac{1}{\omega C} \tag{2.26}$$

Using the load resistance for which the maximum power was found in equation 2.24, the peak power for different resistive loads is the following:

$$|P| = \frac{|V|^2 R}{R_{max\ power}^2 + R_L^2} \tag{2.27}$$

The voltage in the equation is the voltage of the ideal voltage source in the circuit, and is difficult to measure with very low power. An estimate can be made by comparing the voltage as the load resistance increases to a theoretical value.

$$V_R = \frac{V_{ideal} R}{\sqrt{R_{max\ power}^2 + R_L^2}} \tag{2.28}$$

2.4 Conventional energy harvesting systems

The shape an energy harvesting system takes depends in large part upon what manner of energy collection mechanism it relies on. Some energy sources, like solar power, are harvested in a manner that provides direct current. Others, like vibration energy or rain cells, provide an alternating current. The energy of an alternating current can not be stored directly in a battery or a capacitor. Systems utilizing these energy sources therefore need to rectify the AC into DC before storage.

Some systems use the harvested energy instantaneously, for example a bike light powered by the rotation of the wheels. If the wheels stop turning, the light goes off. However, if the power source is inconsistent and the system is intended to deliver power regularly, the energy needs to be stored. Typically this is done with a battery or a large capacitor.

The voltage and current delivered by the energy harvester is not always at a practical magnitude. A single photovoltaic cell provides less than a volt, while certain piezoelectric transducers can provide thousands of them. Electrical devices are usually powered at a certain voltage, and can malfunction or be destroyed by too low or too high voltages. There are a few different methods of converting voltages to other magnitudes without significant power loss. Additionally, the voltage needs to be regulated in the case of variation in the available power and variable loads.

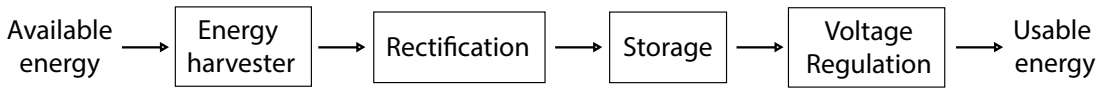

FIGURE 2.9: Energy harvesting system

2.4.1 Rectification

Rectifying an AC signal means that a voltage that alternates between negative and positive values is converted into only positive values. Typically, this is done with diodes. Diodes are semiconductor devices that allow current to flow easily in one direction, but not in the other direction. Figure 2.10 shows the most common diode configurations for rectifying a signal. Realistic diodes introduce a voltage drop in the circuit. Often, as in the figure below, this is modeled as a single voltage typically

around 0.7 V, and the diode will only start conducting if the voltage across it is greater than this threshold voltage. Shockley's diode equation is a better if more complicated model, and figure 2.11 shows how it models a diodes current-voltage relationship.

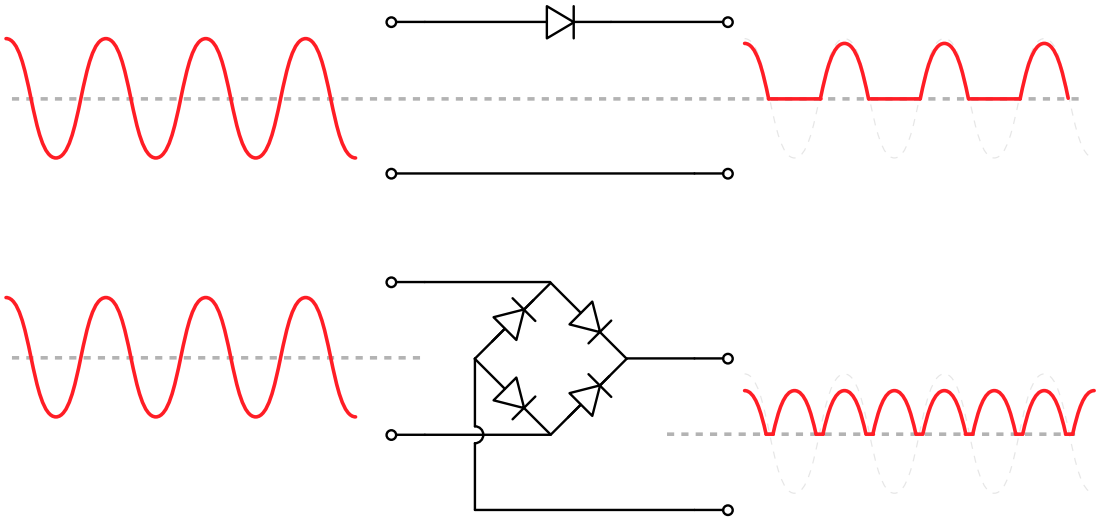

FIGURE 2.10: Single diode and full bridge rectification

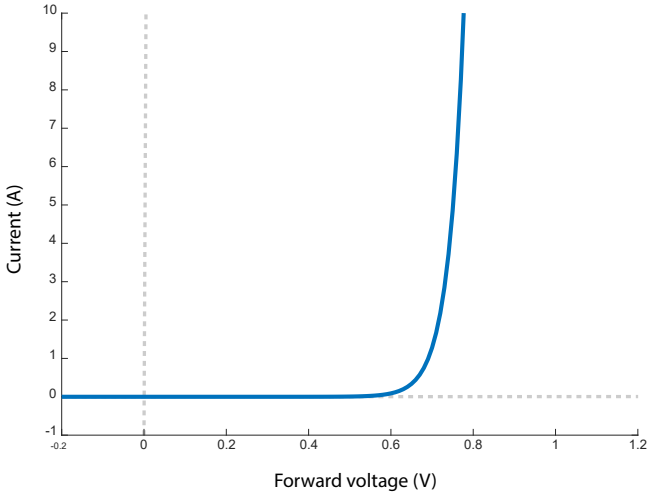

FIGURE 2.11: I-V characteristics of a diode

Shockley diode equation:

$$I_D = I_S\left(e^{\frac{V_D}{nV_T}-1}\right) \tag{2.29}$$

I_D = Current through diode

I_S = Reverse bias saturation current

V_D = Forward voltage

n = Ideality factor

V_T = Thermal voltage

Single diode rectification discards the negative parts of the signal and only allows positive values through. Full bridge rectification inverts the negative parts of the signal so more power is transferred. This is however offset by requiring twice the voltage drop of a single diode rectifier.

Mitigating the voltage drop can be done by employing schottky diodes, which have a lower intrinsic voltage drop, or by using active rectification, in which field effect transistors are used for the rectification [25].

2.5 Storage

The simplest way to harvest rain cell energy is to rectify the the alternating current with a diode bridge, and storing it directly in a capacitor.

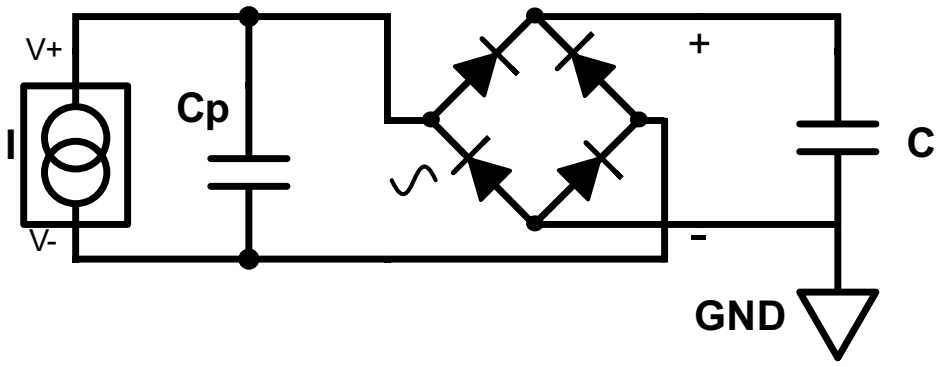

FIGURE 2.12: Bridge rectifier with storage capacitor

In this configuration, the only controllable variable is the capacitance of the storage capacitor C_p. In the manner described in [26], the voltage over the storage capacitor can be regarded as constant over a cycle, as it will change at a much slower rate than the incident voltage waveform.

Current will only flow into the storage capacitor if the voltage output from the rain cell is larger than the voltage over the storage capacitor. Modeling the voltage drops over the diodes as constant, the following condition needs to be true for current to flow: $|V_{out} + 2V_d| < V_p$.

V_d is the diode forward voltage, V_p is the voltage over the rain cell, and V_{out} is the voltage over the storage capacitor. It is assumed that for some time T_2, this is true and the current is flowing, and for some T_1 the capacitor voltage is too high, and the only current is leakage current flowing backwards through the diodes. $T_1 + T_2 = T$ is the total time for the charge from one droplet to be introduced to the circuit.

The average current in the circuit during T is

$$\langle i_{out} \rangle = \frac{1}{T} \int_0^T i(t)dt = \frac{1}{T} \left(0 + \frac{1}{T} \int_{T_1}^{T_2} i(t)dt \right) = \frac{Q_2}{T} \tag{2.30}$$

During period $T2$, V_{C_p} is equal to $V_C + 2V_d$, and Q_2 is the charge transferred to the storage capacitor. During T_1, some charge Q_{1a} goes into C_p, while some $Q_{1b} = i_{leak}T$ leaks through the diodes. The current into C_p can be integrated to find the charge lost in the capacitor.

$$Q_{1a} = \int_0^{T_1} i(t)dt = C_p \int_{-(2V_d+V_{out})}^{2V_d+V_{out}} dV_p = 2C_p(2V_D + V_{out}) \tag{2.31}$$

$$Q_1 = Q_{1a} + Q_{1b} = 4V_D + 2V_{out} + i_{leak}T \tag{2.32}$$

$$\langle i_{out} \rangle = \frac{Q - Q_1}{T} = \frac{Q - 2C_p(2V_D + V_{out}) - i_{leak}T}{T} \tag{2.33}$$

We assume the storage capacitor will increase its voltage in accordance with the average current supplied to it every cycle.

$$\langle i_{out} \rangle = C\frac{dV_{out}}{dt} = \frac{Q - 2C_p(2V_D + V_{out}) - i_{leak}T}{T} \tag{2.34}$$

Solving for voltage:

$$V_{out}(t) = V_0 \left(1 - \exp\left(-\frac{t}{\tau_C}\right)\right) \tag{2.35}$$

$$V_0 = \frac{Q}{2C_p} - 2V_D - \frac{i_{leak}T}{2C_p}$$

$$\tau_C = T\frac{C}{2C_p}$$

If a finite load is connected in parallel with the storage capacitor, that loss must be taken into consideration.

$$\langle i_{out} \rangle = C\frac{dV_{out}}{dt} = \frac{Q - 2C_p(2V_D + V_{out}) - i_{leak}T - \frac{V_{out}T}{R_{load}}}{T} \tag{2.36}$$

In this case the solution takes the same form, but the constants are somewhat different.

$$V_{out}(t) = V_0 \left(1 - \exp\left(-\frac{t}{\tau_C}\right)\right)$$

$$V_0 = \frac{QR_{load} - 4C_P R_{load} V_D - i_{leak} R_{load} T}{T + 2C_P R_{load}}$$

$$\tau_C = \frac{CR_{load}T}{T + 2C_P R_{load}}$$

It can be seen that as R_{load} approaches infinity, the expression for τ_C nears the expression in equation 2.35.

Additionally, if $C_P << C$, the expression for τ_C is approximately equal to $R_{load}C$.

If the diode leakage is modeled as a regular resistance:

$$V_0 = \frac{R_{tot}(Q - 4C_P V_D)}{T + 2C_P R_{tot}}$$

$$\tau_C = \frac{CR_{tot}T}{T + 2C_P R_{tot}}$$

where

$$R_{tot} = \frac{R_{diode}R_{load}}{R_{diode} + R_{load}}$$

The discharge of the circuit follows the pattern of an RC circuit.

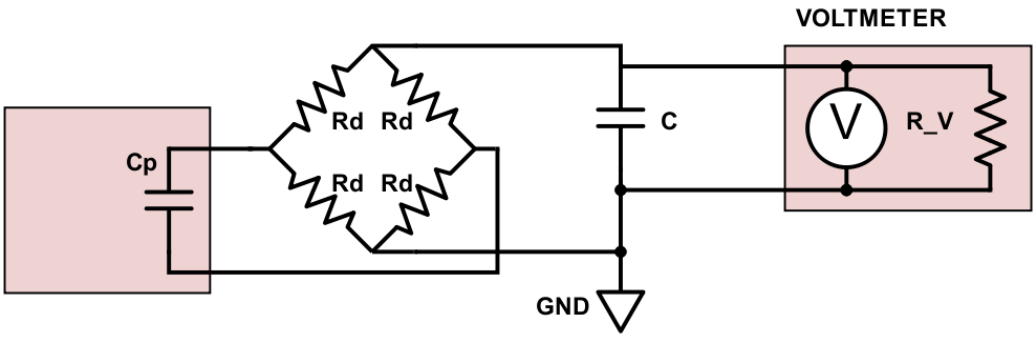

FIGURE 2.13: Diode leakage modeled as high value resistors

$$\frac{V_{out}}{R_{tot}} = C\frac{dV_{out}}{dt} \tag{2.37}$$

$$V_{out}(t) = V_{out}(0)\exp\left(-\frac{t}{R_{tot}C}\right) \tag{2.38}$$

Chapter 3

Experimental setup

3.1 Power measurement

As triboelectric material for the rain droplets, a 25 um thick fluorinated ethylene propylene (FEP) polymer film is used. Interdigitated nickel electrodes of 80 nm thickness are evaporated onto the back-side of the FEP using an electron-beam evaporator located at the nanolaboratory at the Department of Physics and Technology,

External electrical wires were connected to the electrodes using conducting glue or tape. Each electrode had nine fingers that interdigitated with the other electrode. In respect to figure 2.6, D was 2.5 mm, and d was 2.0 mm. The drop radius was estimated to be about 2.8 mm.

The rain cell was mounted underneath a nozzle which continuously dropped droplets onto it from a height of 36 cm. For a period of 1 minute, droplets were allowed to fall onto the raincell at a rate of 2.5 droplets per second. The droplets were about 0.093 mL apiece, and slid down into a glass beaker. A pump continuously pumped the water from the beaker up to the nozzle so as to ensure a continuous dripping.

The electrodes were connected to a test resistor, and the voltage and current were measured simultaneously using a picoammeter and voltage probes. As the droplets deposited negative charge on the polymer, the reservoir in the beaker would get positively charged over time, functioning somewhat like a Kelvin water dropper. This increased the current generated by the rain cell, but as this phenomenon does not occur when ordinary rain falls on a rain cell, both the beaker and the nozzle were grounded to remove any additional charge.

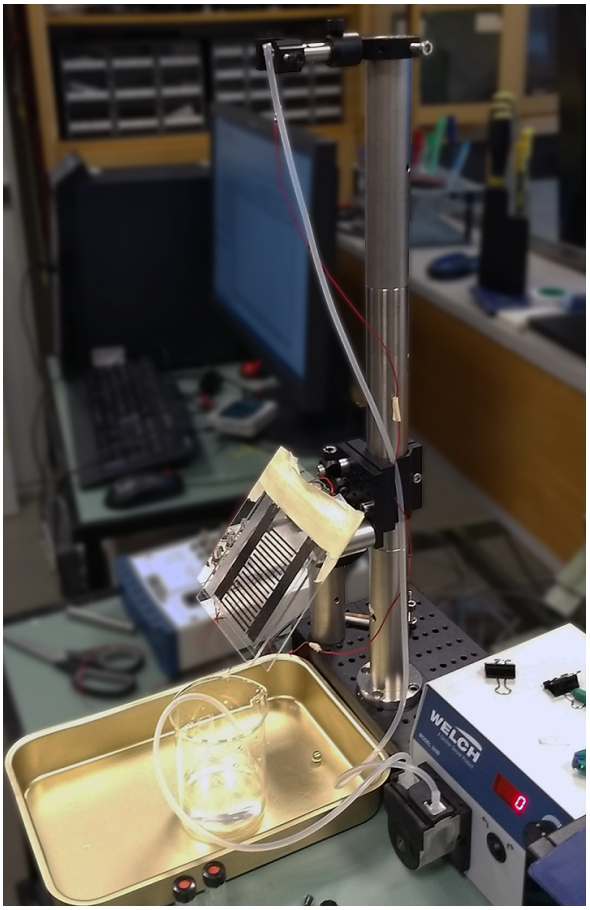

FIGURE 3.1: Experimental setup

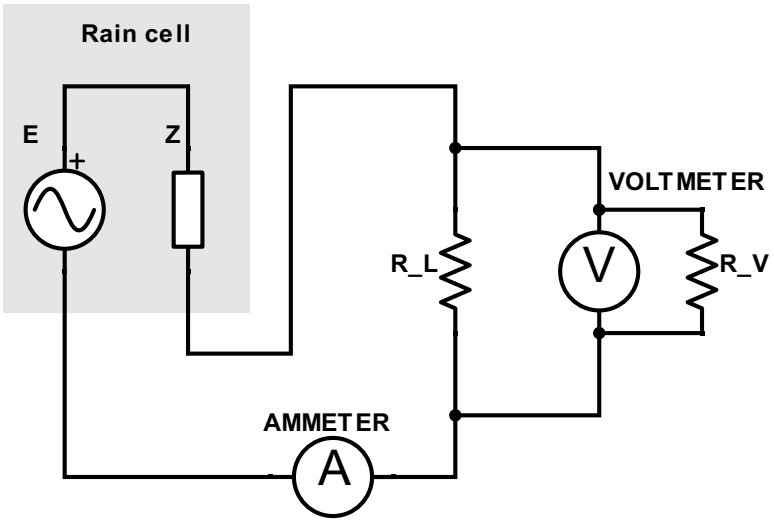

FIGURE 3.2: Power measurement

3.1.1 Equipment

- Keithley 6485 Picoammeter: The current reading was converted to a voltage signal on the analog output, which in turn was read with the Vernier probe.
  - Current reading uncertainty for range 2 μA: $\pm(0.15\% + 100\ pA)$
  - Analog output uncertainty: $3\ \% \pm 2\ mV$.
- Vernier Differential Voltage Probe
  - Resolution: $3.1\ mV$
- Vernier LabQuest Mini
- Resistors of different values
  - Tolerance: $\pm 1\%$

The measurement was repeated for different test loads. Seeing as every droplet left an unique waveform, the power was calculated using an average of the highest peaks achieved per droplet. The whole experiment was run again on two different days to see eventual day to day variations.

The 50 Hz power line noise was reduced with a zero phase digital IIR bandstop filter (figure 3.4).

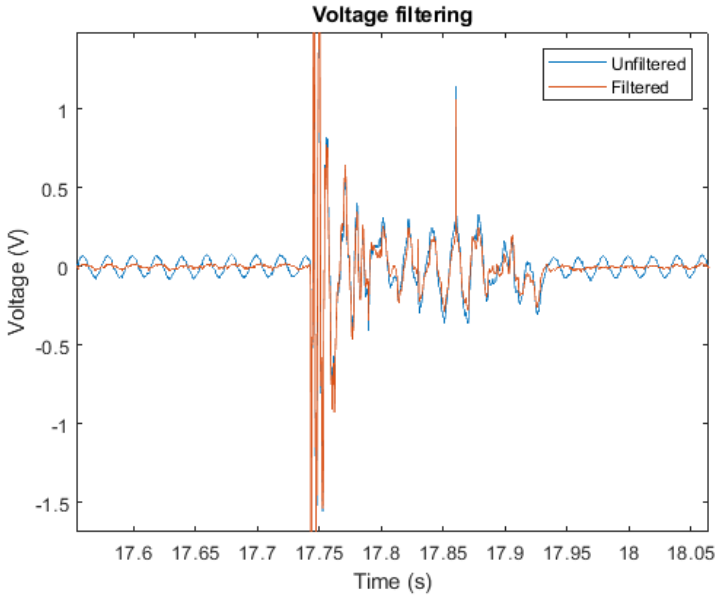

FIGURE 3.4: Measured waveform before and after filtering

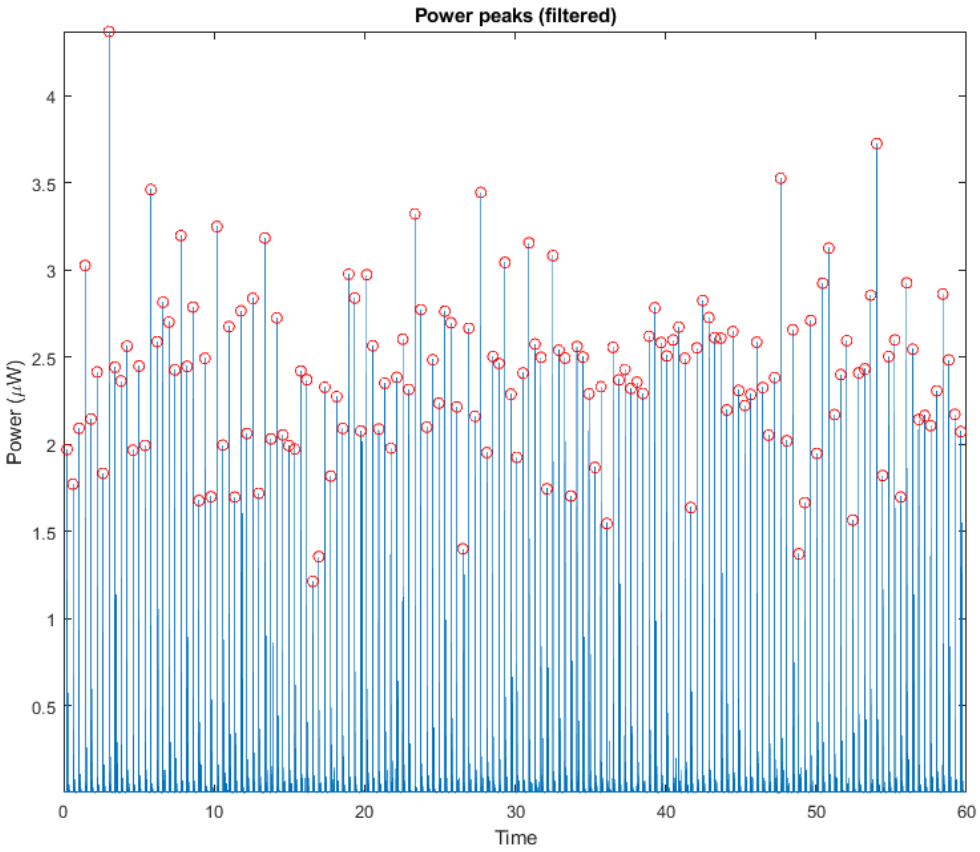

FIGURE 3.3: Each droplet provides a power peak (indicated with red), here with an effective load of 4 megaohms.

3.2 Full wave rectifier

The same rain cell was used in this experiment. The droplets were dripping onto the rain cell from a height of 36 cm. The rain cell was angled at 45 degrees. Droplets were dropped onto the rain cell at a rate of 2.5 droplets every second. The current waveform generated by the rain cell was rectified through the diode bridge, and the storage capacitor was charged. The voltage over the storage capacitor was measured over time. When the voltage had leveled off, the pump was turned off and the capacitor was allowed to discharge without adding any additional load.

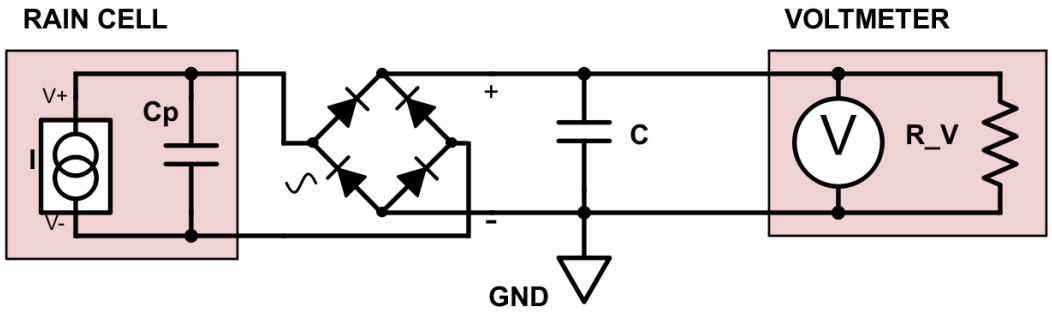

FIGURE 3.5: Voltmeter measuring the voltage over the storage capacitor

3.2.1 Equipment

- Vernier Differential Voltage Probe
  - Resolution: $3.1\ mV$
- Vernier LabQuest Mini
- $10\ \mu F$ electrolytic capacitor
- ON Semiconductor 1N3595 diodes [27]
  - Reverse current for 125 V: max 1 nA
  - Forward voltage: < 0.68 V

Chapter 4

Results

Uncertainties for the measurements in this chapter were calculated in the manner described in appendix A.1.

4.1 Waveform

Figure 4.1 depicts the electrical waveform produced by two droplets. They are characterized by an initial rapid oscillation with a higher amplitude which comes from the droplet impacting the rain cell surface and flattening out over the electrodes. Then the signal transitions to a slower oscillation of lower amplitude as the droplet slides down the rest of the rain cell.

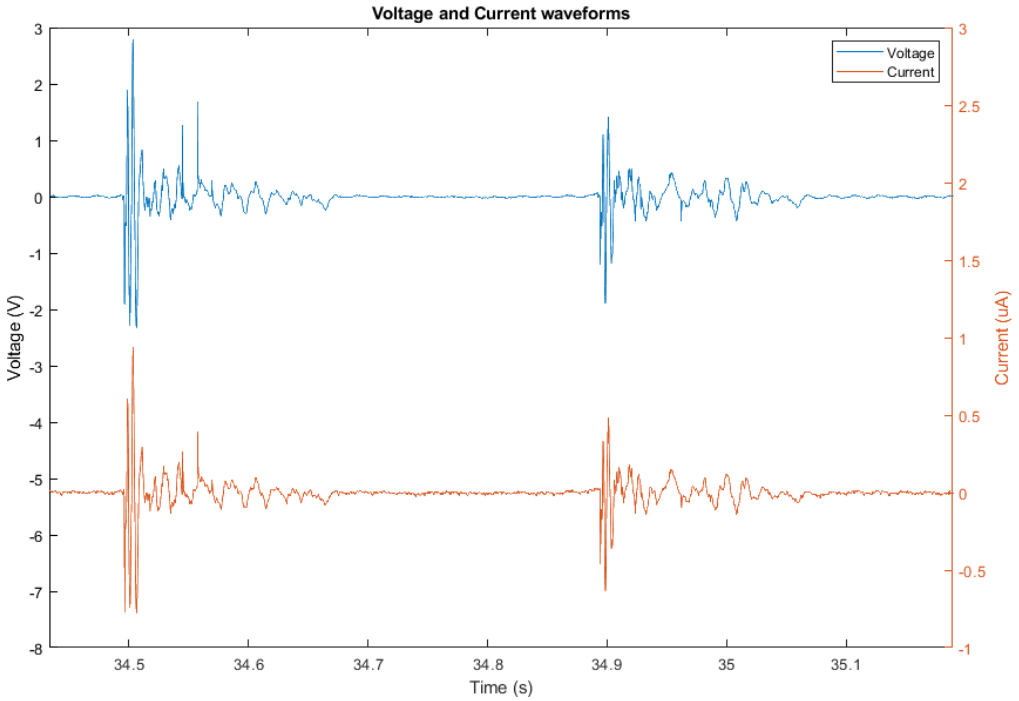

FIGURE 4.1: Sample voltage and power measurements for two droplets

By lowering the nozzle all the way down to the rain cell, the impact oscillations were minimized and the waveform of the droplet sliding down the polymer were emphasized. Here the voltage signal of an open circuit voltage is compared to equation 2.14.

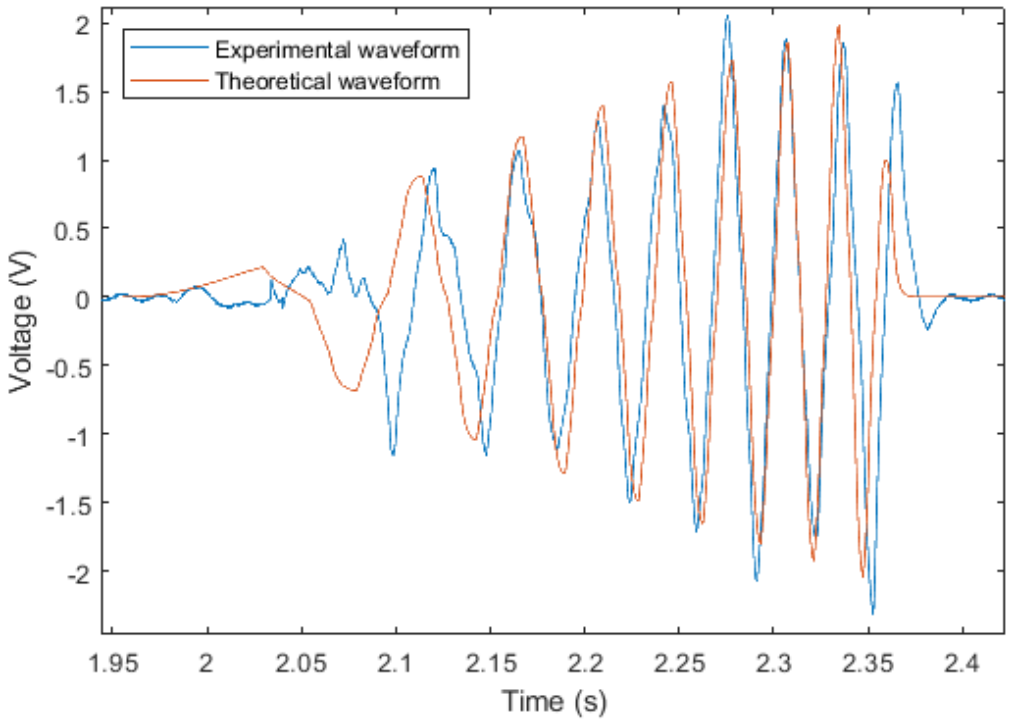

FIGURE 4.2: Experimental and theoretical waveform superimposed

The parameters used for fitting were the coefficient of charge transfer or charge density σ, and the constant $\xi = v(t)/t$.

$$\xi = g(\sin\theta - \mu\cos\theta) \tag{4.1}$$

A ξ of 0.91 was used in the equation. An angle between 5 and 10 degrees give a coefficient of friction between 0.8 and 0.06 which is not entirely unreasonable. citation The charge density was set to 0.00006. Good? Bad?

The experimental signal fits nicely with the theoretical waveform for parts of it, however in the beginning the theoretical waveform lags behind the experimental one. There are a few possible explanations for this. The droplets were pumped onto the rain cell with a pump, and so there was a force in addition to gravity acting on the force at the very beginning of the run. Additionally, with the polymer simply glued onto a piece of plastic, there are inherent differences in the surface topology with small creases and raised areas which can introduce unpredicted results.

4.2 Maximum power

Voltage and current were measured over time as droplets fell onto the rain cell. Power was calculated as the product of voltage and current. Each droplet had a

power peak as the droplet first struck the polymer. These peaks were chosen as basis for the power measurement for a couple of reasons.

Firstly, it is assumed that the capacitance of the rain cell doesn't remain constant throughout the process. The droplet changes shape as it hits the rain cell, and it changes its location relative to the electrodes. An unchanging capacitance is however preferable as it allows for simpler modeling. With some loss of precision, an "effective capacitance" can be found and utilized in modeling and analysis. With the goal being to extract as much power as possible from the rain cell, it is natural to measure the capacitance where the most energy is generated.

$$E(t) = \int_0^t P(t)dt \tag{4.2}$$

As evident from figure 4.3, almost all the generated energy is produced in the initial high power impact, while the energy produced as the droplet rolls down the rest of the rain cell is much lower.

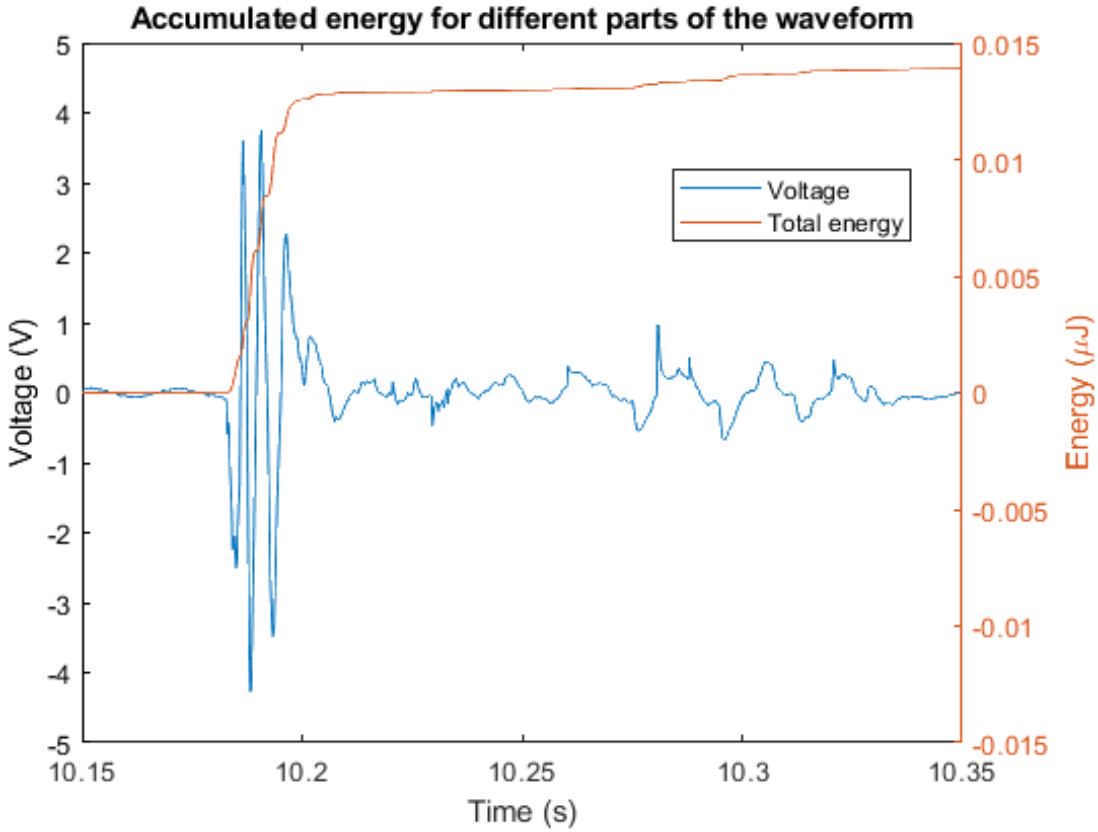

FIGURE 4.3: A sample droplet waveform, load resistance is $4M\omega$.

Secondly, in the sixty seconds the droplets were dropping onto the rain cell, droplets were actually on the rain cell for less than half that time. The breaks between droplets took up most of the time. Therefore, averaging the power produced

would have given a result dependent on the droplet duty cycle which was arbitrarily set in the pump.

The average peak voltage and current measurements were calculated as follows: Peaks were detected from the absolute value of the voltage waveform. The mean of these peak values was recorded below in table 4.1 and 4.2 for each of the load resistances. They are also displayed in graph form in figures 4.4a and 4.4b.

TABLE 4.1: Average peak voltage measurements

		Peak voltage (V)		
Load resistance ($M\Omega$)	Calculated resistance ($M\Omega$)	First series	Second series	Third series
1.1	0.99 ± 0.01	1.34 ± 0.02	1.26 ± 0.02	1.31 ± 0.02
2.5	2.00 ± 0.04	2.32 ± 0.03	2.10 ± 0.03	2.16 ± 0.02
4.3	3.01 ± 0.09	3.16 ± 0.04	2.92 ± 0.04	2.73 ± 0.03
6.6	4.0 ± 0.2	3.71 ± 0.03	3.47 ± 0.04	3.10 ± 0.03
9.91	5.0 ± 0.2	4.16 ± 0.04	3.78 ± 0.05	3.36 ± 0.03
14.894	6.0 ± 0.4	4.40 ± 0.04	4.04 ± 0.05	3.54 ± 0.04
23.612	7.0 ± 0.5	4.57 ± 0.03	4.39 ± 0.06	3.64 ± 0.03
39.76	8.0 ± 0.6	4.63 ± 0.03	3.49 ± 0.06	3.70 ± 0.03
90.082	9.0 ± 0.8	4.75 ± 0.04	3.29 ± 0.05	3.63 ± 0.03
Inf	10 ± 1	4.90 ± 0.03	2.41 ± 0.05	3.28 ± 0.03

TABLE 4.2: Average peak current measurements

		Peak current(μA)		
Load resistance ($M\Omega$)	Calculated resistance ($M\Omega$)	First series	Second series	Third series
1.1	0.99 ± 0.01	1.07 ± 0.01	1.05 ± 0.02	1.16 ± 0.01
2.5	2.00 ± 0.04	0.90 ± 0.01	0.96 ± 0.01	1.01 ± 0.01
4.3	3.01 ± 0.09	0.77 ± 0.01	0.96 ± 0.01	0.90 ± 0.01
6.6	4.0 ± 0.2	0.64 ± 0.01	0.93 ± 0.02	0.82 ± 0.01
9.91	5.0 ± 0.2	0.537 ± 0.005	0.87 ± 0.02	0.77 ± 0.01
14.894	6.0 ± 0.4	0.453 ± 0.004	0.80 ± 0.01	0.74 ± 0.01
23.612	7.0 ± 0.5	0.381 ± 0.003	0.80 ± 0.02	0.69 ± 0.01
39.76	8.0 ± 0.6	0.329 ± 0.003	0.67 ± 0.01	0.66 ± 0.01
90.082	9.0 ± 0.8	0.296 ± 0.004	0.62 ± 0.01	0.62 ± 0.01
Inf	10 ± 1	0.287 ± 0.005	0.47 ± 0.01	0.56 ± 0.01

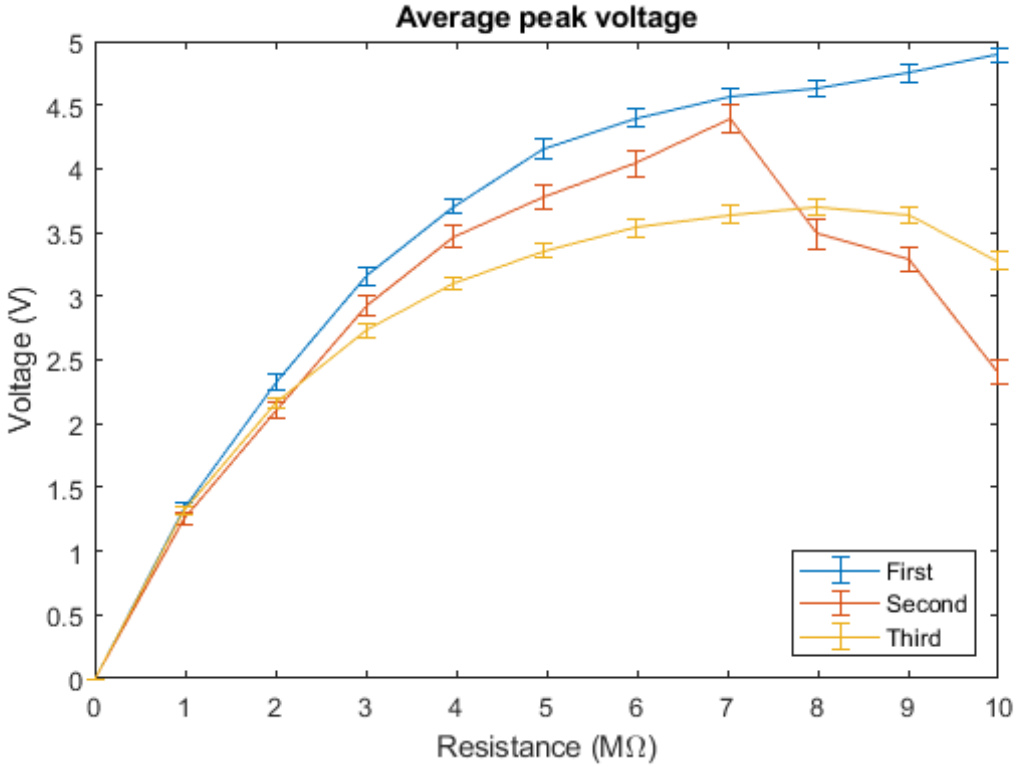

(a) Three different series of voltage peaks

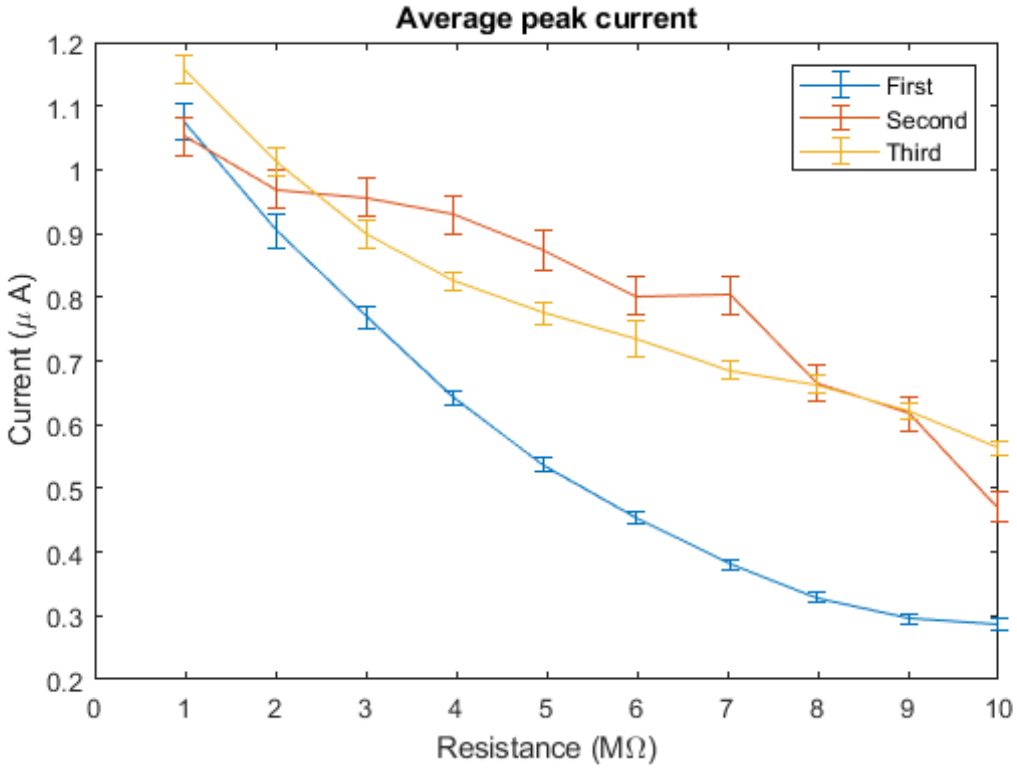

(b) Three different series of current peaks

FIGURE 4.4: Voltage and current peaks measured for different resistive loads

It is evident that something happens with the voltage in the second series. The voltage rises in an expected manner for higher resistances until it reaches seven megaohms. From there the voltage readings take a sharp turn downwards. this behaviour is not consistent with expectations. Assuming the resistances are correct, another variable must have changed. In 2.14, the voltage depends on the quantity σ, which is a proportionality factor that encompasses the charge density in the polymer. The charge density of the polymer sinking could explain the voltage drop. In the paper by Yatsuzuka et al. [20], it is reported that the charge amounts of both the polymer and the droplet decrease as the conductivity of the water increases. While the water in the experiment was initially purified, it was subjected to impurities in the atmosphere throughout the duration of the experiment. The same water was recycled into a open container from which the droplets were pumped up again. As the experiment was conducted by increasing the load resistance for each subsequent run, it would make sense for the voltage to drop towards the high side of the resistance axis. Little consideration was taken towards keeping the time between runs constant, so the drop could very well be abrupt.

Another possibility is that moisture found its way behind the rain cell and between the electrodes. The experiment naturally included some water splashing, and while there was some rudimentary shielding to protect the edges of the rain cell, it was not waterproof. Water seeping into the rain cell could provide an alternate electric path which would lower the effective load resistance and thus also the voltage measured.

The power was calculated by multiplying all the voltage measurements with the current measurements and detecting the peaks. As the load is resistive, current peaks and voltage peaks occur at the same time, and so do also the power peaks.

TABLE 4.3: Average peak power measurements

		Peak power (μW)		
Load resistance ($M\Omega$)	Calculated resistance ($M\Omega$)	First series	Second series	Third series
1.1	0.99 ± 0.01	1.43 ± 0.07	1.35 ± 0.09	1.53 ± 0.07
2.5	2.00 ± 0.04	2.1 ± 0.1	2.1 ± 0.1	2.22 ± 0.09
4.3	3.01 ± 0.09	2.5 ± 0.1	2.9 ± 0.2	2.5 ± 0.1
6.6	4.0 ± 0.2	2.40 ± 0.08	3.2 ± 0.2	2.51 ± 0.09
9.91	5.0 ± 0.2	2.24 ± 0.08	3.2 ± 0.2	2.48 ± 0.09
14.894	6.0 ± 0.4	1.96 ± 0.07	3.1 ± 0.2	2.5 ± 0.2
23.612	7.0 ± 0.5	1.65 ± 0.05	3.4 ± 0.2	2.2 ± 0.1
39.76	8.0 ± 0.6	1.37 ± 0.04	2.2 ± 0.2	2.16 ± 0.08
90.082	9.0 ± 0.8	1.19 ± 0.04	1.9 ± 0.1	1.94 ± 0.07
Inf	10 ± 1	1.10 ± 0.04	1.1 ± 0.1	1.59 ± 0.06

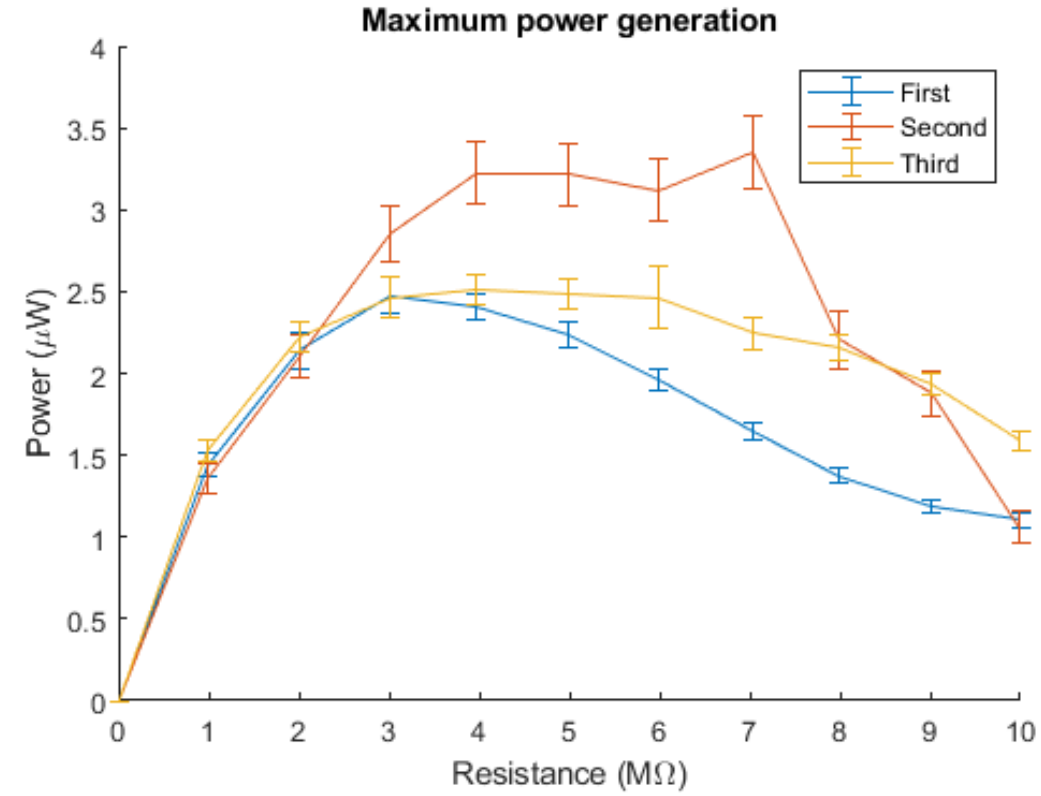

(a) Power at peaks

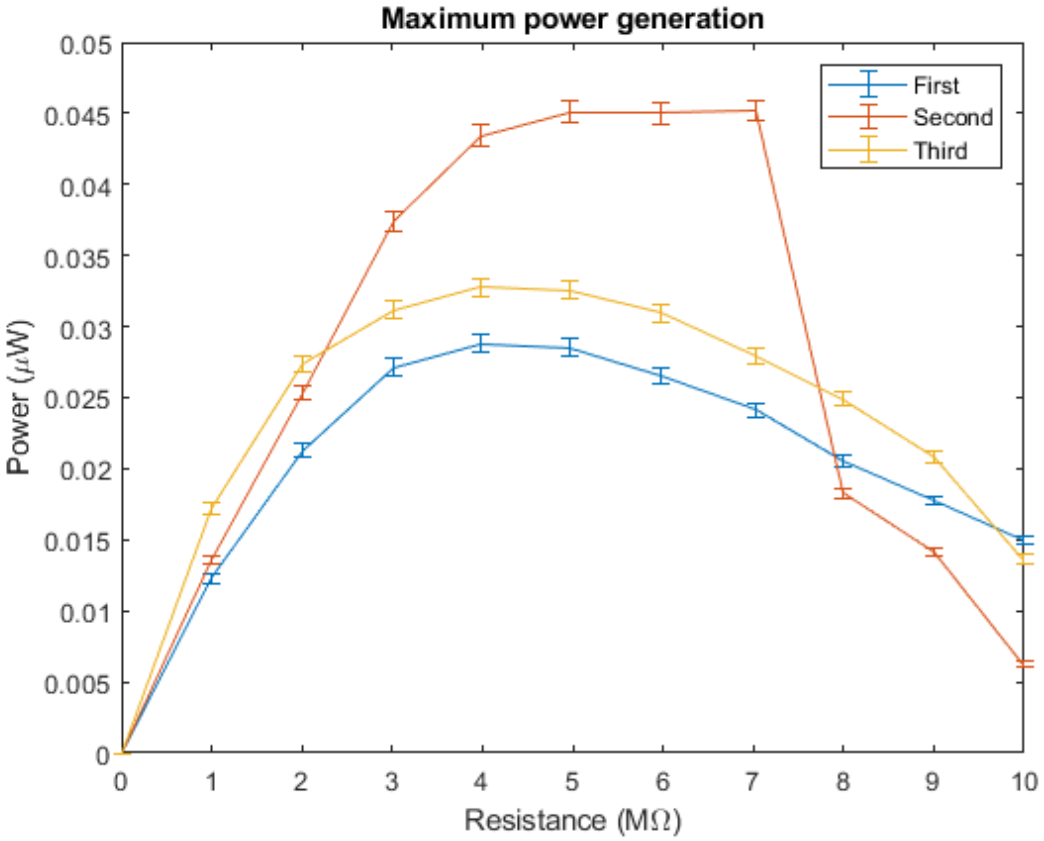

(b) Power in general

FIGURE 4.5: power generation for different resistive loads, first for the peak power production for each droplet, and then the average power for the whole period (not only the peaks). This second plot includes the time between droplets, and may therefore be somewhat misleading.

In both figures it is evident that

TABLE 4.4: Three day mean

Load resistance ($M\Omega$)	Calculated resistance ($M\Omega$)	Peak power (μW)
1.1	0.99 ± 0.01	1.4 ± 0.1
2.5	2.00 ± 0.04	2.2 ± 0.1
4.3	3.01 ± 0.09	2.6 ± 0.3
6.6	4.0 ± 0.2	2.7 ± 0.7
9.91	5.0 ± 0.2	2.7 ± 0.8
14.894	6.0 ± 0.4	2.5 ± 0.9
23.612	7.0 ± 0.5	2 ± 1
39.76	8.0 ± 0.6	1.9 ± 0.7
90.082	9.0 ± 0.8	1.7 ± 0.6
Inf	10 ± 1	1.3 ± 0.4

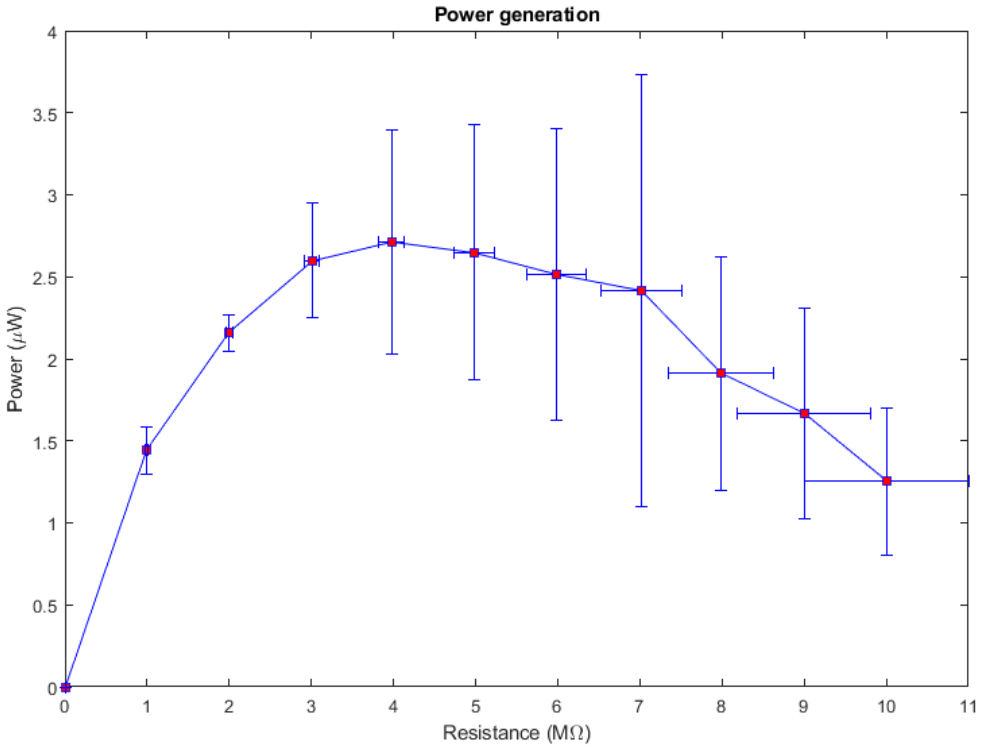

FIGURE 4.6: Power generation for different resistive loads

The true voltage is estimated using equation 2.28. Using a $R_{max\ power}$ of 4 MΩ and adjusting the voltage, an ideal voltage of 4.8 V was found to fit well with the

curve. For higher resistances the voltage dropped, which is evidence of some of the higher resistance measurements not being in line with the rest.

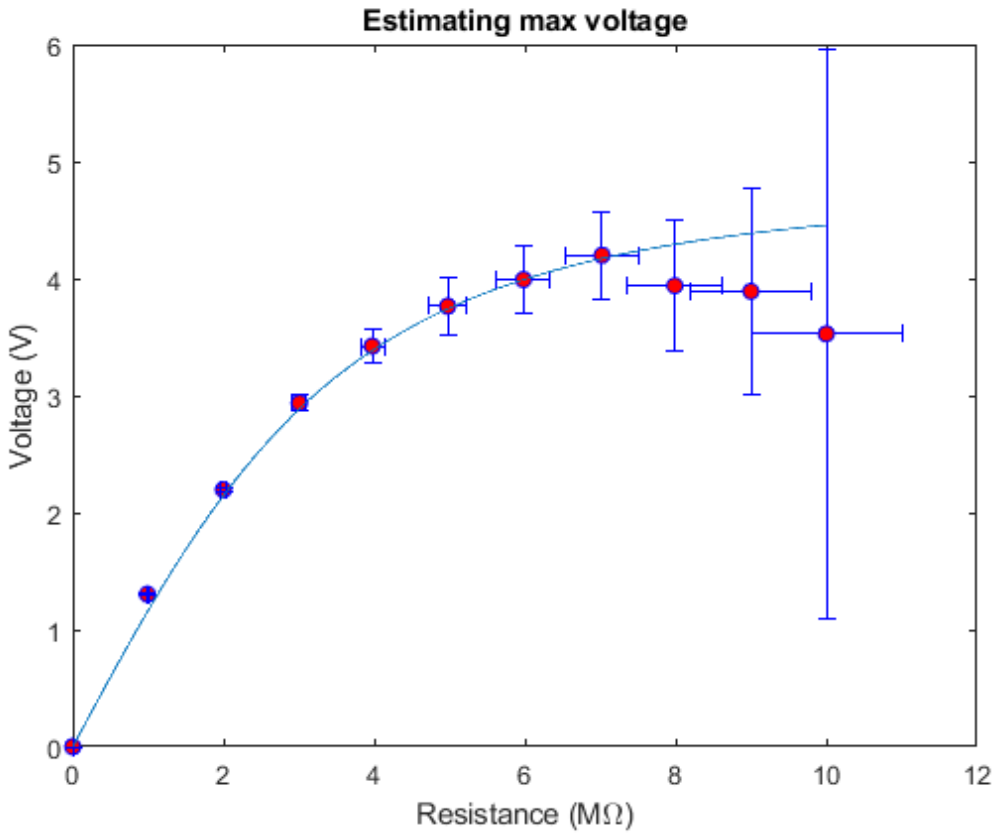

FIGURE 4.7: Estimating the true voltage value

Using this voltage in equation 2.24:

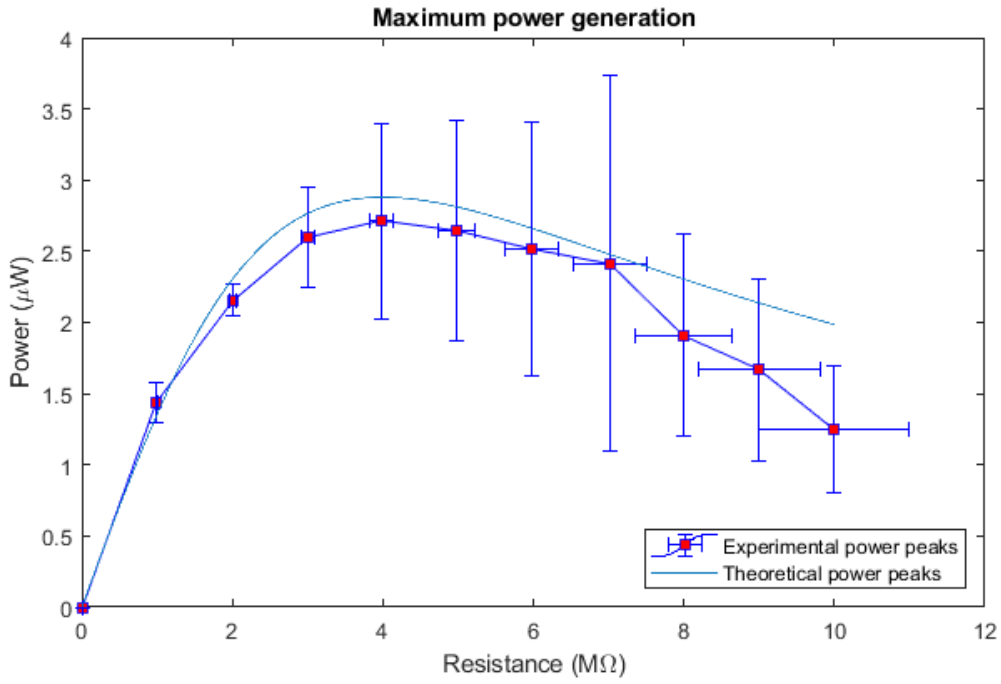

FIGURE 4.8: Comparing theoretical and experimental values for peak power

The highest power transfer measured was 2.7 microwatts, and it was achieved with a resistive load of about 3 - 5 megaohms. At this load, the average energy per droplet is about 0.014 microjoules. This is more than the 1.5 nanojoules that was achieved by Yang, Halvorsen and Dong [11] when rolling mercury drops on similar FEP-covered interdigitated electrodes, however, the comparison is not entirely fair as the mercury drops were merely rolling back and forth on a rotating cell, while these water droplets are dropped from a height.

Wijewardhana et al. [28] had a comparable device (WMAT) that achieved similar results as we have achieved here. Using a fresh PTFE surface, the energy they recorded was around 10 nanojoules per droplet for a wetted polymer. However, using a PTFE surface rubbed with cotton, they achieved a much higher charge density, and consequently the energy per droplet was about 6 times that of the steady state untreated PTFE. This effect did not last over time however, and the rubbed surface dropped down to the level of the untouched surface within two days.

Having learned the resistance for which the power output is greatest, equation 2.26 should tell us the effective capacitance C_P of the rain cell model.

$$C = \frac{1}{\omega R_{max\ power}}$$

A problem arises since the droplet signal does not have a singular frequency. As observed in figure 4.9, the signal slows down as the droplet flattens out. For the sake of simplicity, this can be regarded as a single decreasing frequency, and the average frequency over the high power part of the waveform can be used in further calculations.

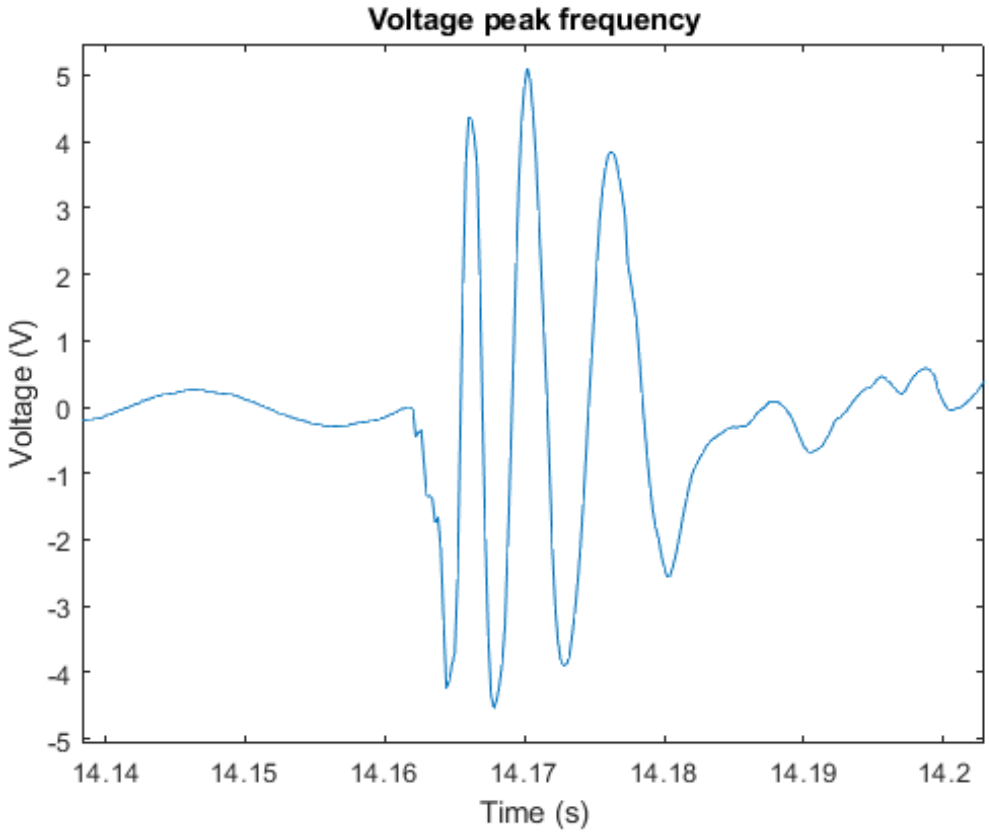

FIGURE 4.9: The initial impact generates the greatest amount of voltage. This part of the waveform has some different frequency components

In this case:

$$\omega = 2\pi \frac{\#\ cycles}{time} = 2\pi \frac{3}{14.1786 - 14.1620} = 1135.5 \tag{4.3}$$

Sampling several different droplets shows that the angular frequency typically is in the range of 1000 - 2000. With a $R_{max\ power}$ of $4\ M\Omega$, this gives a capacitance range of 0.25 to 0.125 nanofarad.

4.3 Charging bridge rectifier

Derive charge transfer

The discharge curve was fit using equation 2.38 and the parameters $V_{out}(0)$ and R_{tot}. The best fit was achieved for a load resistance of 21 megaohms. With a storage capacitance of $10\mu F$, this gives a τ_C of 210.
With the rated leakage of the diodes being less than 1 nA, this leakage is two orders of magnitude smaller than the current through the voltmeter, hence it is difficult to distinguish it from the graph.

Equation 2.35 was fit to the charging curve with the parameters V_0 and τ_C. Since the value for C_P is five orders of magnitude lower than that of C, the time constant for the charging curve is $R_{tot}C$, which is the same as for the discharge curve. With a V_0 of 0.81 V, this fit well with the charging curve.

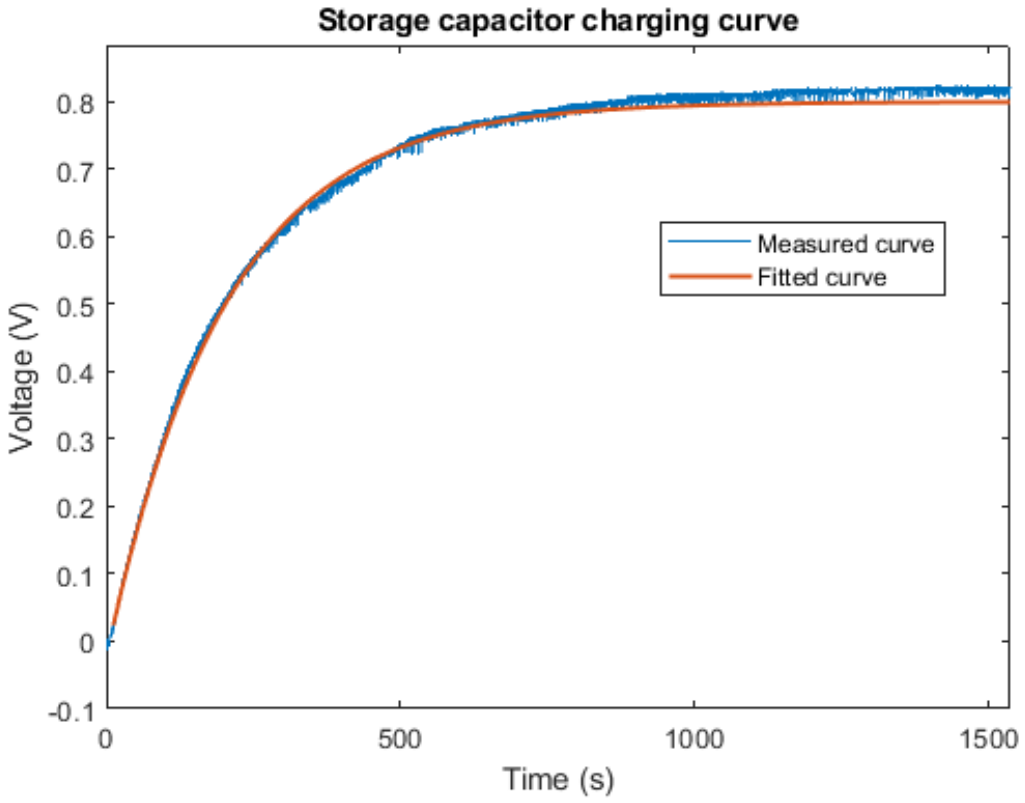

FIGURE 4.10: Bridge rectifier circuit charging a 10 μF capacitor

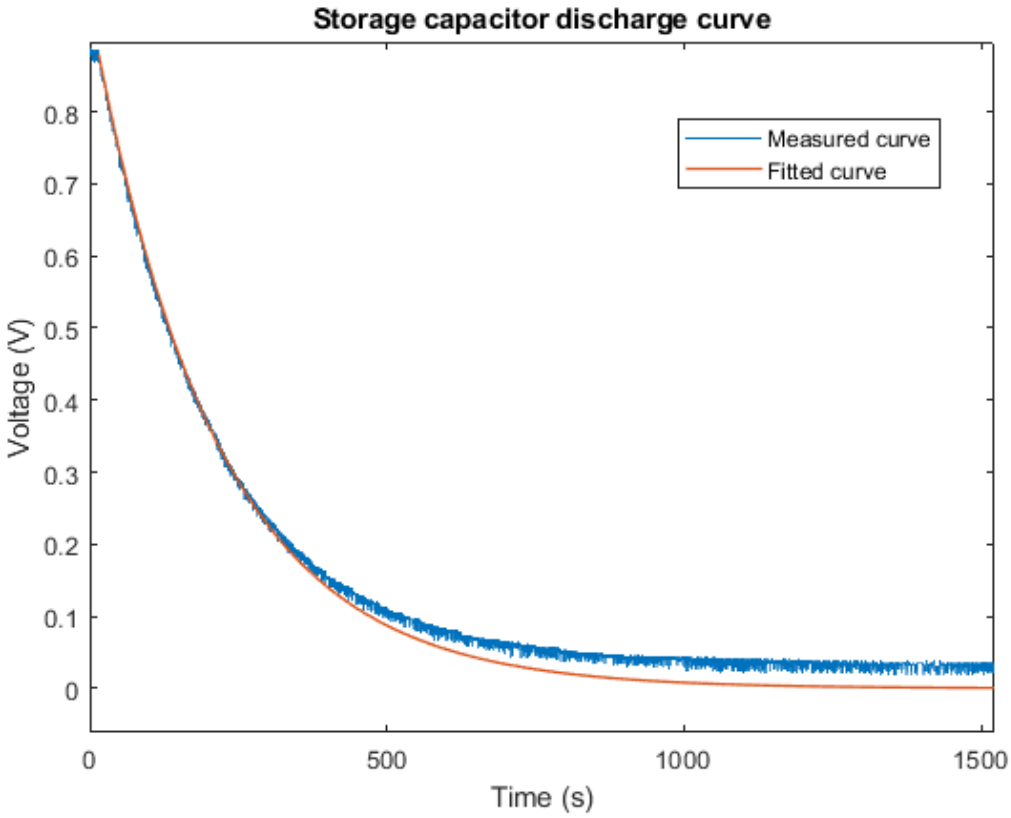

FIGURE 4.11: A 10 μF capacitor being discharged

Solving for Q, equation 2.36 gives the following:

$$Q = \frac{V_0 T + 2C_P R_{tot} V_0 + 4C_P R_{tot} V_D}{R_{tot}} \tag{4.4}$$

$$V_0 = 0.81\ V$$

$$C_P = 0.2\ nF$$

$$R_{tot} = 21\ M\Omega$$

$$V_D = 0.68\ V$$

$$T = 0.4\ s$$

The value of C_P is an estimate from section 4.2. T is the period from which one droplet drops until the next one. This gives a total charge of 16 nC per droplet. In comparison, the charge on the storage capacitor in its steady state was $V_0 \cdot C = 8.1\mu C$. As each droplet only spent 0.155 seconds on the rain cell, this amounts to an average current of $0.1\mu A$ as the droplet is active.

Chapter 5

Discussion

5.1 Energy harvesting potential

The average power a rain cell can provide then depends on the rain intensity. Rain intensity is typically measured in mm/hr, so for a rain cell with effective area A,

$$P_{avg} = \frac{E_{droplet}}{V_{droplet}} \cdot A \cos\phi \cdot R_I \tag{5.1}$$

$$E_{droplet} = \text{Energy of a single droplet}$$

$$V_{droplet} = \text{Volume of a single droplet}$$

$$R_I = \text{Rain intensity}$$

$$\phi = \text{Angle of the rain cell}$$

This simple model does not account for different droplet sizes, velocities, impact location, or the effects of multiple droplets. it is merely intended to give an estimate of the available power.

Considering the rain cell and droplets used in the previous experiment:

$$P_{avg} = \frac{14 \cdot 10^{-9}\,\text{J}}{92.8\,\text{mm}^3} \cdot 4082\,\text{mm}^2 \cdot \cos 45^\circ \cdot \frac{1\,\text{hr}}{3600\,\text{s}} \cdot R_I = 1.2 \cdot 10^{-10} \frac{\text{J hr}}{\text{mm s}} \cdot R_I \tag{5.2}$$

This equals $3.0 \cdot 10^{-8} \cdot R_I$ watts per square meter. It is safe to assume that the characteristics of a rain cell will not remain the same regardless of scale, however, there should be a somewhat equal distribution of simultaneously impinging droplets having destructive or constructive effects on each others waveforms. Capacitance is dependent on area, so the capacitance of the rain cell will most likely change, unless several small rain cells are combined into one big one.

5.1.1 Rain intensity

In order to evaluate the potential of the rain cell as an energy gatherer, it is necessary to consider rainfall statistics in the area of operation. Each droplet deposits a certain amount of energy, and this energy combined with the rate of rainfall and the size of the rain cell gives the continuous energy yield available from rain. However, there are intricacies that make this calculation somewhat more complex.

The following data is taken from eklima.met.no[29]. They display the number of millimetres of precipitation per minute during the year of 2016 at Sandsli observation station. This was the only dataset in the Bergen area covering a whole year without missing time periods. The data was recorded with a pluviometer, which recorded the minute whenever a new tenth of a millimetre of rain had fallen through it. This method caused certain gaps where the rain intensity was lower than the resolution of 0.1 mm/minute. These gaps were filled in with PCHIP (piecewise cubic hermite interpolating polynomial) interpolation. Figure 5.1 shows the cumulative rainfall for the entire year.

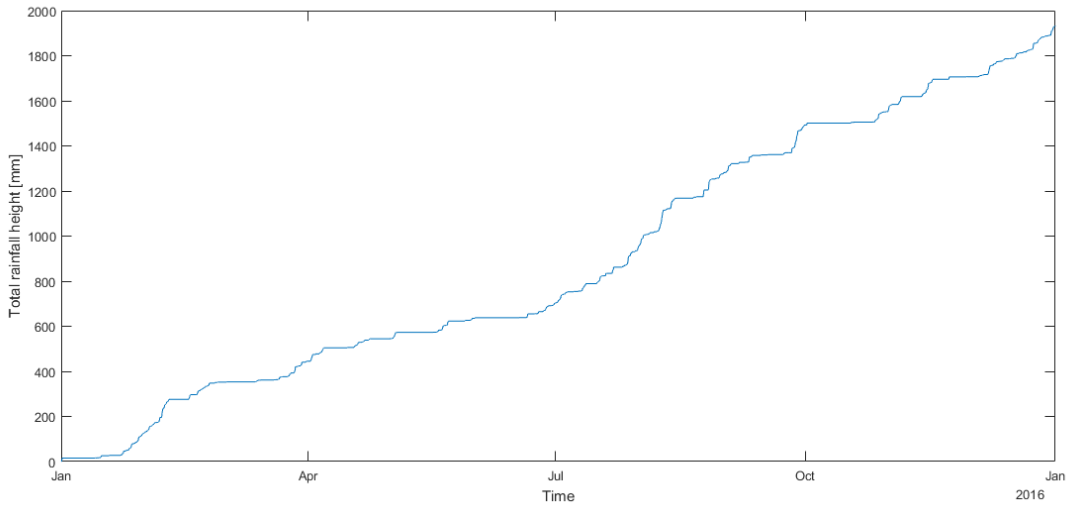

FIGURE 5.1: The total rainfall during the year of 2016

The rain intensity is the time derivative of this function. It is displayed in figure 5.2. The resolution of the data leads to artifacts in the data for multiples of 60 * 0.1 mm/minute.

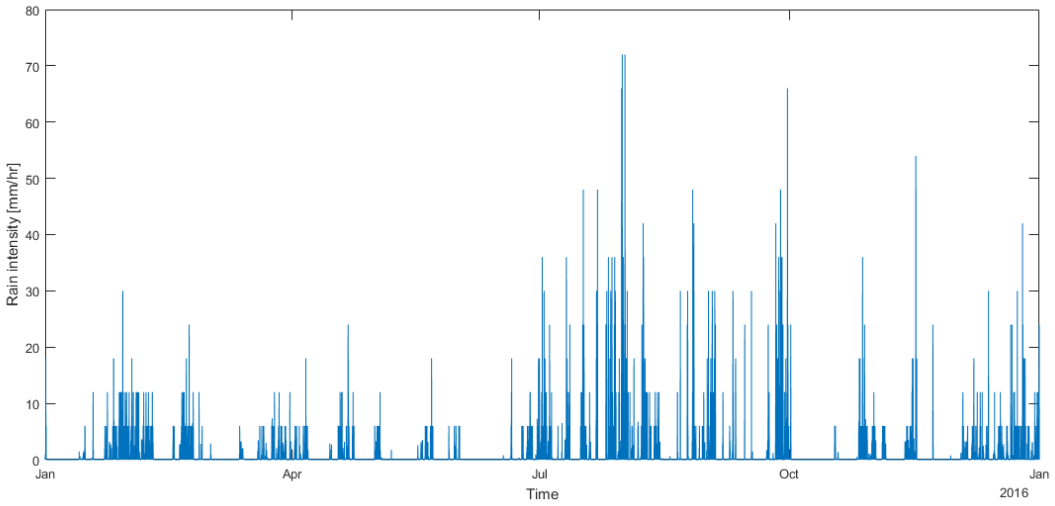

FIGURE 5.2: Rain intensity during the year of 2016

For 2016, the average rain intensity for a single day was 0.44 mm/hr. Looking only at the days with rain, the average was 0.78 mm/hr. Using equation 5.2 for a small rain cell, this amounts to 0.053 nW and 0.094 nW, respectively. Per square meter it amounts to 13 nW and 23 nW.

5.2 Leakage

5.2.1 Diode leakage

Ideally, once the energy was stored, it would remain there until it was needed. Unfortunately, real diodes and capacitors have characteristics that make this difficult. While diodes will block most of the current going the wrong way, there will still be a small leakage current finding its way through. This is evident from the diode equation (Eq. 2.29). In circuits with relatively high voltages and currents, a submicroampere leakage current will usually be of little consequence. In a rain cell system however, the loss is much closer to the levels of current produced, and so it needs to be accounted for in the design.

Figure 5.3 shows the current through three different commercial diodes for different DC voltages.

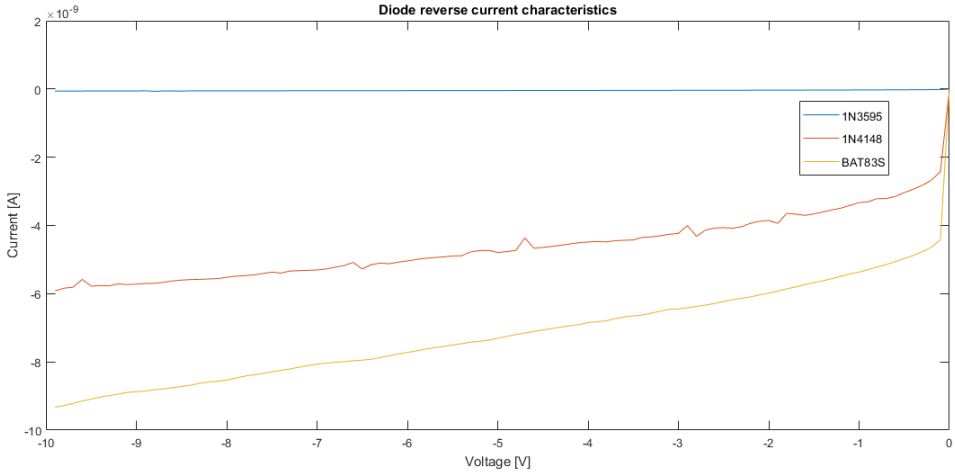

FIGURE 5.3: I-V characteristics for reverse biased diodes

For reverse voltages over a volt, the I-V relationship can be approximated as a linear function, which makes calculations easier.

Model of reverse biased current

5.3 Bridge rectifier

Discuss the theoretical limits that the leakage imparts on the circuit.
As discussed in section 2.5, the steady state voltage of the storage capacitor, and consequently its contained energy, is limited by the amount of charge produced by the rain cell, the internal capacitance of the rain cell, the voltage drop over the diodes, the load, and the leakage through the diodes. When conducting the bridge rectifier experiment, this steady state voltage was 0.81 V. Using the values obtained in that experiment, the voltage for a circuit without load can be estimated. Equation 2.35 shows that for an ideal circuit without leakage or voltage drops, the steady state voltage would be:

$$V_0 = \frac{Q}{2C_P} = \frac{16\ nC}{2 \cdot 0.2\ nF} = 40\ V$$

Two voltage drops of 0.68 V each bring this down to 38.64 V. The leakage is a little more complicated, as it depends on the droplet duty cycle. As an example, we can assume that the time between droplets is twice that of the droplets time on the rain cell. The final voltage would then be

$$V_0 = 38.64\ V - \frac{i_{leak}T}{2C_P} = 38.64\ V - \frac{1\ nF \cdot 2 \cdot 0.155\ s}{2 \cdot C_P} = 37.87$$

Evidently, the effects of such a low leakage are small at this duty cycle. At lower rain intensities, it has a greater bearing on the energy storage, and naturally if the rain stops the leakage will eventually drain the storage capacitor.

Using rain statistics in a similar manner as in section 5.1, the duty cycle is dependent on the rain intensity.

$$dc = \frac{T_{active}}{T_{total}} = T_{droplet}\frac{N_{droplets}}{t} = T_{droplet}\frac{R_I A\cos\phi}{V_{droplet}} \tag{5.3}$$

$dc =$ Duty cycle

$N_{droplets} =$ Number of droplets

$t =$ Time

$T_{droplet} =$ Time the droplet spends on the rain cell

$V_{droplet} =$ Volume of a single droplet

$R_I =$ Rain intensity

$A =$ Rain cell area

$\phi =$ Angle of the rain cell

$$dc = \frac{T_{droplet}}{T} \qquad \Rightarrow \qquad T = \frac{T_{droplet}}{dc} \tag{5.4}$$

Inserting the expression for duty cycle in equation 2.35:

$$V_0 = \frac{Q}{2C_p} - 2V_D - \frac{i_{leak}T_{droplet}}{2C_P dc} \tag{5.5}$$

$$V_0 = \frac{Q}{2C_p} - 2V_D - \frac{i_{leak}V_{droplet}}{2C_P R_I A\cos\phi} \tag{5.6}$$

Using the typical rain intensities from section 5.1.1, 0.44 mm/hr average and 0.78 mm/hr average for rainy days, the following values for the steady state voltage is achieved:

$$V_0 = \frac{16\ nC}{2\cdot 0.2\ nF} - 2\cdot 0.68\ V - \frac{1\ nA}{2\cdot 0.2\ nF}\frac{9.28\cdot 10^{-8}\ m^3}{0.004082\ m^2\cos(45)R_I} = -840\ V \tag{5.7}$$

Obviously, the voltage will not really reach such low limits. It is a consequence

of the leakage being treated as a constant current. In reality, the current would stop as the voltage approached zero. Nevertheless, this means the average rainfall is not sufficient to sustain a voltage with leakage of this magnitude over time. The voltage may build up over shorter periods with heavy rain, but unless it is used, it will leak away. To sustain a 5 V voltage a rain intensity of 11.5 mm/hr is needed, which is quite a lot, even for Bergen. This can be mitigated by using a larger rain cell. Increasing the area of the rain cell would increase the deposited charge, and increase the number of droplets that fell onto the rain cell. Even keeping the deposited charge the same, an area of $0.107\ m^2$ is sufficient to keep all voltage from seeping away, giving a steady state voltage of 5V.

The time constant τ_C is a measure of how long it takes for the storage capacitor to fully charge. The capacitor will charge to within 1 % of its final value within 5 τ_C [30]. The value of this time constant is described by equation 2.35. Substituting equation 5.4 into it, we get

$$\tau_C = \frac{T_{droplet}}{dc}\frac{C}{C_P} = \frac{C}{C_p}\frac{V_{droplet}}{R_I A \cos\phi} \tag{5.8}$$

A larger storage capacitance means slower charging, while higher rain intensity and a larger rain cell speeds it up. A larger internal capacitance also lowers the time constant, but at the price of a lower steady state voltage. The storage capacitor is required to have a certain amount of capacitance determined by the usage it is intended for. For instance, running a Microchip ATtiny1634 microcontroller for one second requires 0.36 mJ of energy [31]. For a given V_0, the energy stored in the capacitor at full voltage is

$$U = \frac{1}{2}CV_0 \tag{5.9}$$

Assuming a voltage regulator that can convert voltages without limitations and without loss, and an upper V_0 bound of 5 V, the storage capacitor would need to be at least $2.9 \cdot 10^{-5}\ F$. With voltage regulators typically only a range of voltages are convertable, and there will be some loss in the conversion process. This means that the storage capacitance in practice would need to be somewhat higher.

Using equation 5.8, the time required for such a capacitor to reach a sufficient voltage can be estimated. Using the increased area required to achieve a 5 V steady

state, the time constant is as follows:

$$\tau_C = \frac{2.9 \cdot 10^{-5}\ F}{0.2 \cdot 10^{-9}\ F} \frac{9.22 \cdot 10^{-8}\ m^3}{1.22 \cdot 10^{-7}\ m/s \cdot 0.107\ m^2 \cdot \cos 45^\circ} = 1450000\ s = 405\ hr \quad (5.10)$$

After just under 17 days of average rain intensity, the capacitor would have reached 63.2% of V_0 [30]. To get within 1% would take five times that.

Chapter 6

Conclusion

6.1 Conclusion

The goal of this thesis was to evaluate the potential of rain cells as an energy source, and to explore the mechanism of gathering this energy for use. The first step was to derive the waveform produced by the interdigitated electrode rain cell. As this waveform was very close to sinusoidal, concepts such as impedance and frequency could be applied.

A model of the rain cell consisting of a current source and a capacitor in parallel was utilized, and it was determined that the rain cell would produce the maximum amount of power when its internal impedance was matched with its load. This provided an experimental method of determining the effective impedance of the rain cells internal capacitor.

Then a model was developed that described the charging and discharging of a storage capacitor connected to the rain cell through a rectifying bridge. This model shows the amount of voltage and indirectly energy that it is possible to collect from a rain cell under certain parameters, and it shows how quickly this process happens. Experimentally it could be used to determine the amount of charge produced by each drop hitting the rain cell.

Three experiments were conducted. The waveform model was compared to the actual signal, and was found to fit well. The rain cell power transfer was measured over different resistive loads, and the effective capacitance of the active rain cell was discovered to be about 0.2 nF. A full wave rectifier was connected to the rain cell and rectified the current into a storage capacitor. This charging curve fit well with theory, and the charge induced by a single drop was discovered.

From the values discovered during the experiment it was to some extent possible to extrapolate the limits of the rain cell in a real world scenario. A formula was developed that related rain intensity to the energy production of the rain cell. It was shown that small rain cells of the sort used in the experiment were insufficient when it came to produce and maintain a stored voltage. The diode leakage was too large to overcome without significant sustained downpours. However, increasing the area of the rain cell improved the energy production considerably, and even with the yearly average rain intensity, the maintenance of a usable voltage became possible. The time the rain cell used to charge up the storage capacitor was also related to the rain intensity, although whether or not the times achieved are acceptable or not depends on the intended use. Charging for 85 days just to power a microcontroller for a second may be sufficient in some scenarioes, but if more speed is needed, increasing the rain cell surface area is the best bet.

References

[1] NASA. *About the Space Station Solar Arrays*. 2017. URL: https://www.nasa.gov/mission_pages/station/structure/elements/solar_arrays-about.html (visited on 11/01/2018).

[2] D. M. Rowe. "CRC Handbook of Thermoelectrics". In: CRC Press, 1995. Chap. 2. Thermoelectric phenomena.

[3] José Luis González, Antonio Rubio, and Francesc Moll. "Human powered piezoelectric batteries to supply power to wearable electronic devices". In: *International journal of the Society of Materials Engineering for Resources* 10.1 (2002), pp. 34–40.

[4] Manuel Piñuela, Paul D Mitcheson, and Stepan Lucyszyn. "Ambient RF energy harvesting in urban and semi-urban environments". In: *IEEE Transactions on Microwave Theory and Techniques* 61.7 (2013), pp. 2715–2726.

[5] A Pop-Vadean et al. "Applications of energy harvesting for ultralow power technology". In: *IOP Conference Series: Materials Science and Engineering* 85.1 (2015), p. 012024. URL: http://stacks.iop.org/1757-899X/85/i=1/a=012024.

[6] Feng-Ru Fan, Zhong-Qun Tian, and Zhong Lin Wang. "Flexible triboelectric generator". In: *Nano Energy* 1.2 (2012), pp. 328 –334. ISSN: 2211-2855. DOI: https://doi.org/10.1016/j.nanoen.2012.01.004. URL: http://www.sciencedirect.com/science/article/pii/S2211285512000481.

[7] Zhong Lin Wang. "Triboelectric Nanogenerators as New Energy Technology for Self-Powered Systems and as Active Mechanical and Chemical Sensors". In: *ACS Nano* 7.11 (2013). PMID: 24079963, pp. 9533–9557. DOI: 10.1021/nn404614z. URL: https://doi.org/10.1021/nn404614z.

[8] Zong-Hong Lin et al. "Water–Solid Surface Contact Electrification and its Use for Harvesting Liquid-Wave Energy". In: *Angewandte Chemie International Edition* 52.48 (2013), pp. 12545–12549. DOI: 10.1002/anie.201307249. eprint: https://onlinelibrary.wiley.com/doi/pdf/10.1002/anie.201307249. URL: https://onlinelibrary.wiley.com/doi/abs/10.1002/anie.201307249.

[9] Li Zheng et al. "Silicon-based hybrid cell for harvesting solar energy and raindrop electrostatic energy". In: *Nano Energy* 9 (2014), pp. 291 –300. ISSN: 2211-2855. DOI: https://doi.org/10.1016/j.nanoen.2014.07.024. URL: http://www.sciencedirect.com/science/article/pii/S2211285514001736.

[10] Zong-Hong Lin et al. "Harvesting Water Drop Energy by a Sequential Contact-Electrification and Electrostatic-Induction Process". In: 26 (July 2014).

[11] Zhaochu Yang, Einar Halvorsen, and Tao Dong. "Power generation from conductive droplet sliding on electret film". In: 100 (May 2012), pp. 213905–.

[12] Z. Yang, E. Halvorsen, and T. Dong. "Electrostatic Energy Harvester Employing Conductive Droplet and Thin-Film Electret". In: *Journal of Microelectromechanical Systems* 23.2 (2014), pp. 315–323. ISSN: 1057-7157. DOI: 10.1109/JMEMS.2013.2273933.

[13] L. E. Helseth and X. D. Guo. "Contact Electrification and Energy Harvesting Using Periodically Contacted and Squeezed Water Droplets". In: *Langmuir* 31.10 (Mar. 2015), pp. 3269–3276. URL: http://pubs.acs.org/doi/abs/10.1021/la503494c.

[14] L.E. Helseth and X.D. Guo. "Fluorinated ethylene propylene thin film for water droplet energy harvesting". In: *Renewable Energy* 99 (Dec. 2016), pp. 845–851. URL: http://dx.doi.org/10.1016/j.renene.2016.07.077.

[15] L. E. Helseth. "Electrical energy harvesting from water droplets passing a hydrophobic polymer with a metal film on its back side". In: *Journal of Electrostatics* 81 (Mar. 2016), pp. 64–70. URL: http://dx.doi.org/10.1016/j.elstat.2016.03.006.

[16] L E Helseth and X D Guo. "Hydrophobic polymer covered by a grating electrode for converting the mechanical energy of water droplets into electrical energy". In: *Smart Materials and Structures* 25.4 (2016), p. 045007. URL: http://stacks.iop.org/0964-1726/25/i=4/a=045007.

[17] Guijun Chen et al. "A droplet energy harvesting and actuation system for self-powered digital microfluidics". In: *Lab Chip* 18 (7 2018), pp. 1026–1034. DOI: 10.1039/C7LC01259D. URL: http://dx.doi.org/10.1039/C7LC01259D.

[18] Yuehua Yuan and T. Randall Lee. "Contact Angle and Wetting Properties". In: *Surface Science Techniques*. Ed. by Gianangelo Bracco and Bodil Holst. Berlin, Heidelberg: Springer Berlin Heidelberg, 2013, pp. 3–34. ISBN: 978-3-642-34243-1.

[19] *FEP Handbook*. DuPont. URL: http://www.rjchase.com/fep_handbook.pdf.

[20] Kyoko Yatsuzuka, Yukio Mizuno, and Kazutoshi Asano. "Electrification phenomena of pure water droplets dripping and sliding on a polymer surface". In: *Journal of Electrostatics* 32.2 (1994), pp. 157 –171. ISSN: 0304-3886. DOI: https://doi.org/10.1016/0304-3886(94)90005-1. URL: http://www.sciencedirect.com/science/article/pii/0304388694900051.

[21] Konstantin N. Kudin and Roberto Car. "Why Are Water-Hydrophobic Interfaces Charged?" In: *Journal of the American Chemical Society* 130.12 (2008). PMID: 18311970, pp. 3915–3919. DOI: 10.1021/ja077205t. eprint: https://doi.org/10.1021/ja077205t. URL: https://doi.org/10.1021/ja077205t.

[22] Simona Strazdaite, Jan Versluis, and Huib J. Bakker. "Water orientation at hydrophobic interfaces". In: *The Journal of Chemical Physics* 143.8 (2015), p. 084708. DOI: 10.1063/1.4929905. eprint: https://doi.org/10.1063/1.4929905. URL: https://doi.org/10.1063/1.4929905.

[23] James K. Beattie. "The intrinsic charge on hydrophobic microfluidic substrates". In: *Lab Chip* 6 (11 2006), pp. 1409–1411. DOI: 10.1039/B610537H. URL: http://dx.doi.org/10.1039/B610537H.

[24] Susan Riedel James W. Nilsson. "Electric Circuits". In: ninth. Pearson, 2011. Chap. 4.10 Thevenin and Norton Equivalents.

[25] Y. Sun et al. "An Integrated High-Performance Active Rectifier for Piezoelectric Vibration Energy Harvesting Systems". In: *IEEE Transactions on Power Electronics* 27.2 (2012), pp. 623–627. ISSN: 0885-8993. DOI: 10.1109/TPEL.2011.2162078.

[26] J. Dicken et al. "Power-Extraction Circuits for Piezoelectric Energy Harvesters in Miniature and Low-Power Applications". In: *IEEE Transactions on Power Electronics* 27.11 (2012), pp. 4514–4529. ISSN: 0885-8993. DOI: 10.1109/TPEL.2012.2192291.

[27] *1N3595: High Conductance Fast Diode*. Rev. A. ON Semiconductor. http://www.onsemi.com/, 2002.

[28] K. Rohana Wijewardhana et al. "Hybrid nanogenerator and enhancement of water–solid contact electrification using triboelectric charge supplier". In: *Nano Energy* 52 (2018), pp. 402 –407. ISSN: 2211-2855. DOI: https://doi.org/10.1016/j.nanoen.2018.08.016. URL: http://www.sciencedirect.com/science/article/pii/S2211285518305792.

[29] eKlima. *Observasjonsliste for nedbør per minutt*. Tech. rep. eklima.met.no: Meterologisk institutt, 2018.

[30] Winfield Hill Paul Horowitz. "Art of Electronics". In: third. ISBN 978-0-521-80926-9 Hardback. 32 Avenue of the Americas, New York, NY 10013-2473, USA: Cambridge University Press, 2016. Chap. 1.4 Capacitors and ac circuits.

[31] *8-bit Atmel tinyAVR Microcontroller with 16K Bytes In-System Programmable Flash*. Microchip. https://www.microchip.com/wwwproducts/en/ATtiny1634, 2014.

Appendix A

Estimating measurement uncertainty

A.1 Power measurement

For a single power reading, the power was calculated as the product of the picoammeter and voltage probe values.

The picoammeters standard uncertainty was composed of the measurement accuracy described in the datasheet, the uncertainty of the analog output, and the resolution of the vernier probe. The measurement uncertainty and the analog output uncertainty are both normally distributed with a 95% confidence interval. The resolution of the Vernier probe gives a rectangular uncertainty distribution.

$$u(I) = \sqrt{u_{meas}^2 + u_{a.o.}^2 + u_{res}^2} \tag{A.1}$$

$$\sqrt{\left(\frac{0.0015 \cdot I + 0.0001\ \mu A}{2}\right)^2 + \left(\frac{0.03 \cdot I + 0.002\ \mu A}{2}\right)^2 + \left(\frac{0.0037\ \mu A}{\sqrt{3}}\right)^2} \tag{A.2}$$

The voltage was measured with another Vernier voltage probe.

$$u(V) = u_{res} = \frac{0.0037\ V}{\sqrt{(3)}} \tag{A.3}$$

An individual power calculation $P = VI$ has the following combined uncertainty:

$$u(P) = \sqrt{V^2 u^2(I) + I^2 u^2(V)} \tag{A.4}$$

The uncertainty of the power peak mean for a single load resistance was calculated as the combination of the instrument uncertainty and the standard deviation of the repeated peak measurements.

$$u(P_{mean}) = \sqrt{u^2(P_{inst}) + \frac{s^2(P_i)}{N}} \tag{A.5}$$

$$u(P_{mean}) = \sqrt{\left(\frac{1}{N}\right)^2 \sum_{i=1}^{N} u^2(P_i) + \frac{1}{N(N-1)} \sum_{j=1}^{N} (P_j - \bar{P})^2} \tag{A.6}$$

The measurement was repeated over three days to evaluate day-to-day variations.

$$u(P_{mean(3days)}) = \sqrt{\left(\frac{1}{N}\right)^2 \sum_{i=1}^{N} u^2(P_{mean,i}) + \frac{1}{N(N-1)} \sum_{j=1}^{N} (P_{mean,j} - \bar{P})^2} \tag{A.7}$$

To achieve a 95% confidence interval, the resulting standard uncertainty was multiplied with a cover factor of 2. As the three day mean only had three measurements, a Student's T distribution was used to determine its standard uncertainty.

There was also some uncertainty present in the load resistors. As the voltage probe had an internal resistance comparable to the loads in use, it acted as a separate load wired in parallel. Load resistors were therefore chosen so that the resultant resistor networks amounted roughly to integer values of megaohms.

$$R_{tot} = \frac{R_{load} R_{probe}}{R_{load} + R_{probe}} \tag{A.8}$$

The uncertainty of N resistors with the same relative uncertainty $u_{rel} = \frac{u(R_i)}{R_i}$ in series is calculated as follows:

$$R_{tot} = \sum_{i=1}^{N} R_i \tag{A.9}$$

$$u^2(R_{tot}) = \sum_{i=1}^{N} \left(\frac{\partial R_{tot}}{\partial R_i}\right)^2 u^2(R_i) = \sum_{i=1}^{N} u^2(R_i) \tag{A.10}$$

$$u^2(R_{tot}) = \sum_{i=1}^{N} u_{rel}^2 R_i^2 = u_{rel}^2 \sum_{i=1}^{N} R_i^2 \tag{A.11}$$

$$u^2(R_{tot}) = \left(\frac{u_R}{R}\right)^2 \sum_{i=1}^{N} R_i^2 = u_R^2 \frac{\sum_{i=1}^{N} R_i^2}{\left(\sum_{i=1}^{N} R_i\right)^2} \tag{A.12}$$

$$\frac{\sum_{i=1}^{N} R_i^2}{\left(\sum_{i=1}^{N} R_i\right)^2} < 1 \Longrightarrow u(R_{tot}) < u(R) \tag{A.13}$$

The uncertainty of resistors in series is less than the uncertainty of a single resistor of the equivalent resistance and the same relative uncertainty.

Similarly, for parallel resistors:

$$\frac{1}{R_{tot}} = \frac{1}{R_1} + \frac{1}{R_2} \Longrightarrow R_{tot} = \frac{R_1 R_2}{R_1 + R_2} \tag{A.14}$$

$$u^2(R_{tot}) = \left(\frac{\partial R_{tot}}{\partial R_1}\right)^2 u^2(R_1) \left(\frac{\partial R_{tot}}{\partial R_2}\right)^2 u^2(R_2) \tag{A.15}$$

$$u^2(R_{tot}) = \left(\frac{R_2^2}{(R_1 + R_2)^2}\right)^2 u(R_1)^2 + \left(\frac{R_1^2}{(R_1 + R_2)^2}\right)^2 u(R_2)^2 \tag{A.16}$$

$$u^2(R_{tot}) = \left(\frac{R_2^2}{(R_1 + R_2)^2}\right)^2 R_1^2 \frac{u(R_1)^2}{R_1^2} + \left(\frac{R_1^2}{(R_1 + R_2)^2}\right)^2 R_2^2 \frac{u(R_2)^2}{R_2^2} \tag{A.17}$$

$$u^2(R_{tot}) = \left(\frac{R_2^2 R_1}{(R_1 + R_2)^2}\right)^2 \frac{u(R_1)^2}{R_1^2} + \left(\frac{R_1^2 R_2}{(R_1 + R_2)^2}\right)^2 \frac{u(R_2)^2}{R_2^2} \tag{A.18}$$

$$u^2(R_{tot}) = \left(\frac{R_2 R}{R_1 + R_2}\right)^2 u_{rel}^2 + \left(\frac{R_1 R}{R_1 + R_2}\right)^2 u_{rel}^2 \tag{A.19}$$

$$u^2(R_{tot}) = R^2 u_{rel}^2 \frac{R_1^2 R_2^2}{(R_1 + R_2)^2} \tag{A.20}$$

$$u^2(R_{tot}) = u^2(R) \frac{R_1^2 + R_2^2}{(R_1 + R_2)^2} \tag{A.21}$$

$$\frac{R_1^2 + R_2^2}{(R_1 + R_2)^2} < 1 \Longrightarrow u(R_{tot}) < u(R) \tag{A.22}$$

As this is true for two resistors in parallel, it must necessarily be true for several resistors as well. In the same way, any resistor network of parallel and series resistors with the same relative uncertainty will have lower uncertainty than an equivalent resistor with the same relative uncertainty. For the sake of simplicity, the load resistor networks have therefore been treated as single resistors in this analysis. This choice also counters any correlation that could be present between the separate resistor uncertainties.

The uncertainty of the internal resistance of the voltage probe was not described, so it was estimated to be 10% of its value. The uncertainty for the resultant load of the resistor and the internal resistance of the probe is:

$$u^2(R_{tot}) = \left(\frac{R_{probe}^2}{(R_{load} + R_{probe})^2}\right)^2 u(R_{load})^2 + \left(\frac{R_{load}^2}{(R_{load} + R_{probe})^2}\right)^2 u(R_{probe})^2 \tag{A.23}$$